Physics of Ferronematics with Soft Particle Anchoring

Sergei *V*. Burylov
Transmag Research Institute, Ukrainian Academy of Sciences
Dnepropetrovsk, 320005, Ukraine

Yuri *L*. Raikher
Institute of Continuous Mechanics
Urals Branch of the Russian Academy of Sciences
Perm, 614062, Russia

Received October 4, 1994

We present an extended review on the theory of ferronematics–suspensions of single-domain ferromagnetic particles in liquid-crystalline carriers. The classical continuum theory developed by F. Brochard and P. de Gennes is considered and modified in order to take into account the finiteness of anchoring of the nematic molecules on the particle surfaces. With a number of examples based on the recently published experimental data we show that our model is capable to provide an adequate quantitative description of the equilibrium properties of thermotropic ferronematics.

I. Introduction

Ferronematic liquid *crystals* or *Ferronematics* which hereafter we abbreviate to FN, is the name for suspensions of monodomain ferro- or ferrimagnetic particles in nematic liquid crystals. The most essential feature of these systems is a strong orientational coupling between the disperse phase (ferroparticles) and the liquid-crystalline matrix. The applied magnetic field, changing the orientation of the particles, via them affects the texture of the nematic matrix. Therefore it enables to acquire a full-scale control over the orientational state of FN with the aid of rather weak–much less than 100 Oe–magnetic fields. In the first part of this paper (Sec.II-VII) we highlight the basic concepts of physics of FN, and in the second (Sec. VIII-XI)–use them to interpret some experimental data reported on real thermotropic ferronematic systems.

The idea of creation of artificial anisotropic fluid substances with high sensitivity to a magnetic field had appeared probably in a very short time after thc successful synthesis of colloidal magnetic suspensions in ordinary liquids – *magnetic fluids* – had been firstly performed[1]. The move from isotropic liquid carriers to anisotropic ones, apart from discovery of numerous new physical effects, looks imensely promising from the viewpoint of possible technological applications.

Indeed, nematic liquid crystals (NLC) had proved to be the media with a well-pronounced optical response (birefringence, light scattering) to a variety of externa1 factors – electric fields, flows, stresses, etc. – which provoke distinctive changes in their internal orientational structure. Due to that NIJC are now among the most widely used materials for making up various sensors as well as image processing devices.

As to the magnetic field, the reaction of a pure nematic to its action is relatively weak. The cause is that the orientational ordering of diamagnetic molecules of NLC cannot produce anything but the anisotropy of the diamagnetic susceptibility of the substance. For obvious reasons, this anisotropy χ_a is of the same order of magnitude as that of solid diamagnetic crystals, and being defined per unit volume, is $\chi_a \sim 10^{-7}$. The energy density associated with the diamagnetic term in a

magnetic field H is then $\chi_a H^2$, which amount should be compared to the density of the orientation-elastic interaction of the liquid crystal K/D^2, where K is the characteristic value of the Frank modulus and D is the reference size of a nematic specimen. A simple estimate for $K \simeq 5 \cdot 10^{-7}$ dyn and D $\sim 100\mu$m[2] shows that the magnetic field amplitudes H $\sim \sqrt{K/\chi_a D^2}$ capable to change the orientational texture of nematic, and thus produce a noticeable optical response, range to several hundreds of Oersteds and rapidly grow up to several kOe with the diminution of the specimen size.

Doping a liquid crystal with ferromagnetic admixture (single-domain magnetically hard grains) should impart to it the magnetization $M \simeq \mathbf{I}, f$, where $\mathbf{I},$, is the spontaneous magnetization of the used ferromagnetic material, and f is the volume concentration of the grains. The corresponding contribution to the energy density is I_sf H. Once more comparing it to the orientational-elastic term, we get the estimate

$$H \sim K/I_s f D^2 , \qquad (1)$$

which for $I_s \simeq 5 \cdot 10^2$ G (ferrite) and the former values of K and L, yields H $\sim 10^{-5}/f$. Thus we see that even at rather low volume fractions of particles (f $\sim 10^{-3}$%) the characteristic amplitude of the field, leading to a substantial orientational (and hence optical) response, is two-three orders of magnitude less than that for pure nematics. Note that the field range H $\sim$ 1 Oe indicated by formula (1) is comparable with the natural terrestrial field, so that the latter might play an important role in FN.

From our viewpoint, the above-presented short account of estimates is already a sufficient justification of potential merits of ferronematics. However, the experimental way to their creation was not simple. The first attempt[3] did not give any real proof of success. It had taken about ten years more until FN systems of lyotropic kind were obtained[4]. There the liquid-crystalline phase was formed by orientationally ordered water solution of platelet-like micelles ($\sim$ 30 nm in major size) while the magnetic component was presented by relatively large ($\sim$ 1-10 μm in length) prolate aggregates of ultra-fine ($\sim$ 10 nm) ferroparticles. The aggregates were formed in result of a microscopic phase separation of an ordinary magnetic fluid dissolved in the lyotropic carrier. Those lyotropic FN turned out to be relatively stable and reproducible, and for the first time have provided an opportunity to observe and measure the essentially new properties of liquid-crystalline ferromagnetic dispersions[5–8].

As a matter of fact, the most fruitful directions of the would-be experimental research were outlined yet in 1970 by the pioneering theoretical work of F. Brochard and P. de Gennes[9]. Still now this masterly written paper may serve as a source of inspiration for all newcomers to the field. There the authors had proposed and studied magnetic NLC suspensions, whose solid phase consists of needle- or rod-like ferrite particles with the length L $\gg$ a (where a is the NLC molecule size) and diameter d $\simeq L/10$. Such a distinctive anisometricity imparts to the particles a substantial magnetic rigidity thus making them to be small permanent magnets. The volume fraction f of particles in FN is supposed to be sufficiently small to be able to ignore the interparticle magnetic dipole-dipole interaction. In Ref. [9] there was derived a set of equations of orientational- elastic equilibrium in FN capable to describe large-scale structures of the director field as well as stationary distributions of concentration, magnetization, etc. For a long time the Brochard-de Gennes model was the only existing one, and it had been widely used in explanations of particular effects encountered in FN[5,6,7,8,10–14].

A new line of experimental studies has begun in 1983, when for the first time ferromagnetic dispersions on the base of a thermotropic nematic liquid crystal were prepared[15]. These FN consist of the mesogenic compound MBBA into which, with the aid of a special surfactant, needle-like particles of y-ferric oxide are embedded. The linear size of the particles is about 500nm with the aspect ratio around 7:1. With those thermotropic systems a number of interesting observations and measurements of optical effects was obtained[16–19].

It occurred, however, that the theory[9], never being in serious contradiction with the experimental evidente on lyotropic FN, came to a dead-end when having been applied to thermotropic ones. The most clear and unambigous qualitative proof of this (though not mentioned by the authors) had been given right in the very first paper on thermotropic FN[15]. There is reported an observation of the Fredericksz transition with a threshold of several hundreds of Oe in a FN slab where the applied magnetic field was perpendicular to the unperturbed director of the nematic matrix. However, as it is shown explicitly in Refs. [10, 11], according to the Brochard-de Gennes model in such a situation FN must display an immediate orientational response to the field, i.e., the transition threshold must be exact zero.

This principal contradiction had tempted us to reconsider the basic assumptions of the classical theory[9]. Our work[20–23] hacl yielded that a correct description of the observed behavior of thermotropic FN may be achieved if to turn down just one of the postulates of [9] – the assumption of rigid anchoring of the nematic molecules on the particle surfaces. In fact, the detailed analysis resulted in a size-dependent criterion of applicability of the rigid anchoring approximation, and proved that the latter, being valid for large quasi-grains of lyotropic FN, fails for much smaller particles of thermotropic dispersions.

In a composite medium, which FN actually is, each component–the ferroparticle assembly and the nematic matrix–possesses its own set of the orientational degrees of freedom. So, the form of the equilibrium equations essentially depends upon the origin of coupling between the order parameters of the subsystems. In a magnetized FN, where the parallelicity of the particle axes means, simultaneously, the alignment of their magnetic moments, it is reasonable to characterize tlie state of the orientational order by two intrinsic variables–director $\mathbf{n}(\mathbf{r})$ and local magnetization $\mathbf{M}(\mathbf{r})$–both averaged over a spatial scale large in comparison with the particle size L. Therefore, the macroscopic theory of FN should contain at least one parameter responsible for the local correlation between n and M. From this point of view, the approach proposed in Ref. [9] looks indeed oversimplified, since it takes into account only the asymptotic case of infinitely strong orientational coupling: demanding, instead of a balanced correlation, an invariable parallelicity of n and M.

In Refs. [21, 22] we have demonstrated that the rigid anchoring approximation ($\mathbf{n} \parallel \mathbf{M}$) may be used in FN only if the condition

$$Wd/K \gg 1 , \qquad (2)$$

holds; here W is the surface density of the anchoring energy of the nematic. For the existing MBBA-based FN with the homeotropic surface alignment one should set $W \sim 10^{-3}-10^{-2}$ dyn/cm and $K \approx 5\cdot 10^{-7}$ dyn (see Ref. [24], for example). Substituting this into Eq.(2) together with the given in[15–17] value of the transverse diameter of the particles $d \approx 70$ nm, one gets $Wd/K = 10^{-2} - 10^{-1}$ that is apparently not greatei than unity. In view of Eq. (2), tlie latter estimation proves that tlie rigid anchoring approximation is invalid for thermotropic FN. In below we shall develop a continuum model of FN taking into account the finiteness of the surface energy, i.e., valid for the case $Wd/K \leq 1$.

II. Orientational distortions created by a solid anisometric particle inside a uniform nematic

Although our objective is the development of a macroscopic approach, we have to begin with some single-particle, "microscopic", problems which are of fundamental significance for all the further considerations. As the first step, it is necessary to determine a character of the orientational distortions induced in an anisotropic fluid (NLC) by a suspended object–an individual particle of a suspension. In the rigid anchoring approximation (2) this question had been in detail studied in Ref. [9], but now we need the solutions valid for finite values of W.

Let us consider a solid acircular particle embedded in a uniform nematic domain whose director $\mathbf{n}_0 = const(\mathbf{r})$ is fixed at infinity. We assume that all over the particle surface some definite boundary condition holds.

Since the length L of the magnetic grain is always much greater than the size of the nematic molecules, the particle behaves like a macroscopic object interacting with the director field by the orientational-elastic and surface potentials. The total free energy of the system is then the sum of the corresponding contributions integrated over the sample volume V and the particle surface S, respectively:

$$\mathcal{F} = 1/2 \left[K \int_V (\nabla \mathbf{n})^2 dV + W \int_S \sin^2 \gamma dS \right] \quad (3)$$

Here γ is the angular deviation of the director from its easy-orientation direction on S. Note that writing down Eq. (3) we have made certain conventional simplifications: chosen the surface potential of NLC in the Rapini form (see Refs. [2, 24]), and adopted the single-constant (isotropic) approximation for the elastic energy, i.e., neglected the differences between the Frank moduli K_i setting $K_1 = K_2 = K_3 = K$.

According to usual rules[2], variation of the functional (3) gives the equilibrium equation for the liquid crystal orientation together with the corresponding boundary condition:

$$\nabla^2 \mathbf{n} = 0 , \quad \delta\mathcal{F}|_S = 0 , \quad (4)$$

where $\delta\mathcal{F}|_S$ is the variation of $\mathcal{F}$ on the particle surface. At distances r $\gg$ L, i.e., far from the particle, the latter but weakly disturbs the orientation field. So the solution of Eq. (4) may be presented in the form $\mathbf{n}(\mathbf{r}) = \mathbf{n}_0 + \delta\mathbf{n}(\mathbf{r})$, where Sn $= (\delta n_x, \delta n_y, 0)$ in the coordinate system with the z-axis along $\mathbf{n}_0$. Taking into account the transversality of the perturbation (Sn $\perp \mathbf{n}_0$), one may write it as

$$\delta\mathbf{n} = (\mathrm{O} \times \mathbf{n}_0) , \quad (5)$$

thus introducing an auxiliary pseudo-vector O. According to Eqs. (4)-(5), it has to satisfy the conditions $\nabla^2\Omega_x = \nabla^2\Omega_y = 0$ or the vector Laplace equation

$$\nabla^2 \mathbf{\Omega} = 0 , \quad (6)$$

everywhere inside the liquid crystal volume.

For a non-chiral particle, vector $\mathbf{\Omega}$ vanishing at infinity, expands into inverse power series in r as

$$\mathbf{\Omega} = \frac{q}{r}\mathbf{a} + O\left(\frac{1}{r^2}\right) , \quad (7)$$

where a and q do not depend upon r. The scalar parameter q is determined by the nature of the boundary condition on the particle surface and vector a–by the orientation of the particle relative to the liquid crystal. Then for a we may use the proposed in Ref. [9] representation

$$\mathbf{a} = (\mathbf{n}_0\mathbf{u})(\mathbf{n}_0 \times \mathbf{u})l , \quad (8)$$

where l is a parameter of the dimension of length, and the unit vector $\mathbf{u}$ denotes the direction of the main symmetry axis of the particle. In general, instead of a mere product $(\mathbf{n}_0\mathbf{u})l$, in Eq. (8) one has to write $f(\cos\vartheta)$, where f is some odd function of the argument $(\mathbf{n}_0\mathbf{u}) \equiv \cos\vartheta$. The purpose of the simplification made, which is in fact the replacement of f by just the first term of its expansion in the power series in cos ϑ, is that it is sufficient for the model in question.

In the following it is convenient to choose 1 positive, and describe the possible change of vector $\mathbf{\Omega}$ direction by the change of sign of q. To comply with the choice (8) of a, the "interfacial" coefficient q should be a dimensionless function of the only dimensionless combination available, namely, the ratio

$$\omega = WR/K ,$$

(cf. Eq. (2)), of the reference particle size R to the so-called extrapolation length $b = K/W$ [2] of the liquid crystal. In below we show that for a solid cylinder suspended in a nematic, parameter R coincides with its radius. As to the magnitude of the functiou $q(\omega)$, it is easy to point out to its limiting values: for rigid anchoring $|q(\infty)| = 1$ (see Ref. [9]), and for the entirely degenerated (isotropic) boundary condition $q(0) = 0$. Therefore, it looks reasonable to assume that in the intermediate w range $|q(\omega)| < 1$.

Returning to the solution (5) of the equilibrium equation and substituting therein Eqs. (7) and (8), we may write it in the form of a long-wave distortion

$$\delta\mathbf{n} = \frac{ql}{r}\mathbf{s}\ ,\ \mathbf{s} = (\mathbf{n}_0\mathbf{n})(\mathbf{n}_0 \times (\mathbf{u} \times \mathbf{n}_0))\ . \qquad (9)$$

To understand the meaning of vector **s**, let us consider it under condition of small rotations of the particle $|\delta\mathbf{u}| = |\mathbf{u} - \mathbf{u}_0| \ll 1$ for two possible types of the particle equilibrium orientation. At no || u ~that is the case considered in Ref. [9], when Su ⊥ no, one gets

$$\mathbf{s} = \mathbf{u} - \mathbf{n}_0(\mathbf{n}_0\mathbf{u}) = \mathbf{u}_\perp\ ,$$

where $\mathbf{u}_\perp$ is the component of **u** in the direction perpendicular to $\mathbf{n}_0$ and u ~ Since in this situation $\mathbf{u}_\perp$ is the whole perturbation, it means that s = $\delta\mathbf{u}/$. At $\mathbf{n}_0 \mathbf{I} \mathbf{u}_0$ which, as it would be shown below, is the case for FN with soft anchoring, expansion of **s** with respect to small rotations gives

$$\mathbf{s} = \mathbf{u}_0(\mathbf{n}_0\mathbf{u})\ .$$

The latter vector has the length $|\delta\mathbf{u}|$ but is parallel to $\mathbf{u}_0$ which is now the axis along the Sn direction. From Eq. (9) it is clear also that at rigid anchoring ($|q| = 1$) the role of the distortion amplitude is played solely by l while at finite w, it is reduced by the factor q.

To evaluate the torque exerted on the nematic by the embedded particle with an arbitrary orientation **u**, let us surround the particle by a closed surface C sufficiently remote as to allow the use of the asymptotic formulas (7) and (9) for Ω and Sn. Varying the system free energy (3) and taking into account the equilibrium volume and boundary conditions, we get

$$\delta\mathcal{F} = K\int_\Sigma d\Sigma_i \delta n_k \frac{\partial n_i}{\partial x_k}$$

With the aid of Eq. (9) and the condition $\delta\mathbf{n} \mathbf{I} \mathbf{n}_0$ it transforms into

$$\delta\mathcal{F} = qKl\mathbf{s}\delta\mathbf{n}\int_\Sigma d\Sigma_i \frac{\partial}{\partial x_i}\left(\frac{1}{r}\right) = -4\pi qKl\mathbf{s}\delta\mathbf{n}\ .$$

Hence, the torque exerted on the nematic by the particle may be written as

$$\mathbf{\Lambda} = -\mathbf{n} \times \frac{\delta\mathcal{F}}{\delta\mathbf{n}} = 4\pi qKl(\mathbf{n}_0\mathbf{u})(\mathbf{n}_0 \times \mathbf{u})\ . \qquad (10)$$

If the particle does not experience any additional external force (magnetic, gravitational etc.), then its torque-free static orientation $\mathbf{u}_0$ is determined by condition $\mathbf{\Gamma} = 0$. Eq. (10) provides two choices, viz., $\mathbf{u}_0 \| \mathbf{n}_0$ and $\mathbf{u}_0 \perp$ no. Of the latter, the stable one is selected by the demand that the free energy decrement should be positive, or that the perturbation-induced torque of the nematic matrix should restore the initial state. From Eq. (10) it follows that the actual equilibrium orientation of the particle is determined by the sign of the coefflcient q. For example, at q > 0 it is stable at $\mathbf{u} \| \mathbf{n}_0$ and unstable at $\mathbf{u}_0 \perp \mathbf{n}_0$. Note that neither of these two orientations induce any long-wave distortion: substitution of Eq. (8) into Eq. (10) yields a = 0 at $\mathbf{\Gamma} = 0$. These distortions arise only when there appears some externa1 torque $\mathbf{\Gamma}_{ext}$ acting on the particle. In equilibrium $\mathbf{\Gamma}_{ext}$ is counteracted by the torque - $\mathbf{\Gamma}$ exerted by the nematic on the particle, and the balance condition gives $a = \mathbf{\Gamma}_{ext}/4\pi qK$.

III. Distortion energy

From now on we shall consider a particle in the form of a long cylinder (its length being L and radius R ~ $L/10$) suspended in NLC and assume that the boundary conditions are the same all over the cylinder surface. Let us evaluate the free energy (3) for an arbitrar~orientation of the particle axis relative to the unperturbed director no. Though the exact solution of this problem could be found only for certain particular cases[21,25], it is feasible to obtain a reasonable approximationfor the general one. For this purpose, we need to estimate the volume and surface integrals entering Eq. (3). Doing that, we shall neglect the effect of the end-walls of the cylinder, since their contributions are about R/L times less than that of the lateral surface. Taking into account that in the case of finite anchoring $|\nabla\mathbf{n}| \sim 1/b$ near the particle surface, for the orientational-elastic term we have

$$1/2K\int_V (\nabla\mathbf{n})^2 dV \sim \pi KLR^2(W/K)^2 = \omega^2 \cdot \pi KL\ , \qquad (11)$$

and for the surface contribution

$$1/2W\int_S \sin^2\gamma dS \sim dS \sim \pi WRL = \omega \cdot \pi KL\ . \qquad (12)$$

Comparison of Eqs.(11) and (12) shows that up to the first order of magnitude in parameter $w \ll 1$ (cf. Eq. (2)) the free energy may be replaced merely by its surface term.

Following the approximation $\omega \ll 1$, let us write the director on the particle surface as $\mathbf{n}_S = n + 0 + \delta\mathbf{n}_S$, where $|\delta\mathbf{n}_S| \sim \omega$. Since the surface angle γ entering Eqs. (3) and (12) is defined by relation $\sin\gamma = (\mathbf{n}_{0S} \times \mathbf{n}_S)$ where $\mathbf{n}_{0S}$ is the direction of easy orientation on the particle surface, with the same accuracy we may set $\sin\gamma = (\mathbf{n}_{0S} \times \mathbf{n}_0)$ and thus present the free energy of the particle-induced distortion in the form

$$\mathcal{F} = 1/2W \int_S (\mathbf{n}_{0S} \times \mathbf{n}_0)^2 dS \ . \qquad (13)$$

In the cylindrical coordinate framework fixed on the particle, vectors $\mathbf{n}_0$ and $\mathbf{n}_{0S}$ may be written as

$$\begin{aligned} \mathbf{n}_0 &= (\sin\vartheta, 0, \cos\vartheta) \ , \\ \mathbf{n}_{0S} &= (\sin\alpha\cos\beta, \sin\alpha\sin\beta, \cos\alpha) \end{aligned} \qquad (14)$$

where the angles are defined in Fig.1. Substituting Eqs. (14) into Eq. (13), one gets after integration

$$\mathcal{F} = 1/2\pi\omega KL[1 + \cos^2\alpha - (3\cos^2\alpha - 1)\cos^2\vartheta] \ . \quad (15)$$

Differentiation with respect to the angle ϑ yields the expression for the torque exerted by the particle on the nematic. With the notation $\cos\vartheta = (\mathbf{n}_0\mathbf{u})$ – see Fig.1 – it takes the form

$$\mathbf{\Gamma} = \pi\omega KL(3\cos^2\alpha - 1)(\mathbf{n}_0\mathbf{u})(\mathbf{n}_0 \times \mathbf{u}) \ . \qquad (16)$$

Comparison of Eqs. (10) and (16) shows that for soft anchoring ($\omega \ll 1$) the distortion amplitude l and the "interfacial" coefficient q may be chosen, respectively, as

$$l = L, \quad q = 1/2\omega P_2(\cos\alpha) \ , \qquad (17)$$

where $P_2(\cos\alpha)$ is the second-order Legendre polynomial. Note that the angle α depends solely on the kind of the boundary condition, and for a given material triad *particle substance - surfactant - nematic* may be only but temperature dependent.

The obtained expression for q is useful, in particular, to determine the type of the particle equilibrium orientation. Writing down the difference between the particle energies provided by Eq. (15) in the orthogonal orientations, viz. $\mathbf{u} \parallel \mathbf{n}_0$, and $\mathbf{u} \perp \mathbf{n}_0$, one gets

$$\Delta\mathcal{F} = \mathcal{F}_\parallel - \mathcal{F}_\perp = -2\pi qKL \ . \qquad (18)$$

This formula settles the straightforward way to selection of the stable equilibrium states of the particle. From there it is apparent that it is the sign of the coefficient q, i.e., the orientational pattern of anchoring, which determines the type of equilibrium. As Eqs. (17) show, the sign of q is controlled by the angle α between the easy-orientation direction $\mathbf{n}0S$ and the symmetry axis of the cylinder – see Fig.1 for definition of α. Introducing the reference value $\alpha_* = arccos(1/\sqrt{3})$ so that $P_2(\cos\alpha_*) = 0$, we find that

$$\begin{aligned} &\Delta\mathcal{F} < 0 \quad \text{and} \quad \mathbf{u} \parallel \mathbf{n}_0 \quad \text{for} \alpha < \alpha_* \ , \\ &\Delta\mathcal{F} > 0 \quad \text{and} \quad \mathbf{u} \perp \mathbf{n}_0 \quad \text{for} \alpha < \alpha_* \ . \end{aligned} \qquad (19)$$

Note also that with the aid of formula (18) one may write the orientation-dependent part of the particle energy (15) as

$$\begin{aligned} \mathcal{F}(\vartheta) &= \mathcal{F}_\perp + [\mathcal{F}_\parallel - \mathcal{F}_\perp](\mathbf{u}\mathbf{n}_0)^2, \\ \mathcal{F}_\perp &= -2\mathcal{F}_\parallel = 4\pi qKL/3. \end{aligned} \qquad (20)$$

The existence of a definite preferred orientation of a particle in the nematic matrix is the necessary condition for establishing the orientational coupling in a system like FN. In this context it is worth to remark that the results of Eqs. (19) are valid only if the energy gap $|\Delta\mathcal{F}|$ is greater than the thermal energy k_BT, i.e.,

$$WRL/k_BT \gg 1 \ .$$

Substituting here the reference values of the material parameters of thermotropic FN, we find that at room temperature $WRL/k_BT \sim 10 - -100$. However this condition might break down for too small particles or too low surface energies.

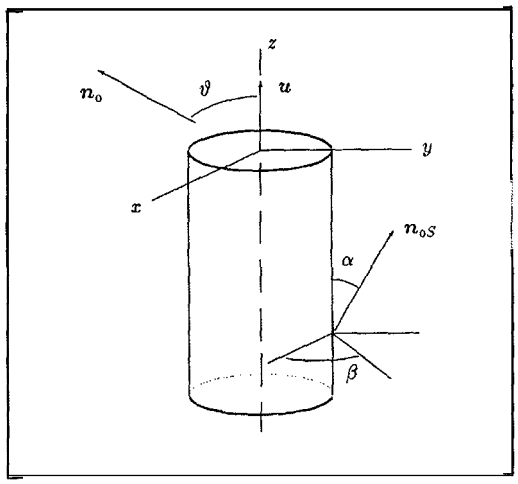

Figure 1: Cylindrical particle suspended in a nernatic; on the choice of the reference angles. Here u is tlie unit vector of the particle major axis, $\mathbf{n}_0$ is the unperturbed director of the nematic domain, $\mathbf{n}_{0S}$ is the easy orientation direction on tlie particle surface, α and β are the angles of $\mathbf{n}_{0S}$ with the axes of tlie coordinate framework whose polar axis lies along u.

IV. Orientational interaction of the particle assembly with the nematic matrix

Let us proceed to the problem of the orientational coupling between the nematic and the particles suspended in it. As it had been shown in Ref. [9], in the systems alike FN, the nematic matrix in response to the unison rotation of the particles might display two types of the orientational behavior. The first one takes place when the number concentration c of the solid phase is lower than some characteristic value c,. Under these circumstances each particle distorts the director field independently of the neigbors, and the deviations between local u and n are great. Due to that, the resulting perturbations but weakly influence the macroscopic striicture of the nematic. Conversely, if the particle concentration exceeds c,, then the response mode known as the *collective behavior*[9] occurs. Upon it, the local orientation deviations of the particles and nematic are close and change smoothly over the FN sample. Only in this case the rotation of particles induces a substantial macroscopic orientational response in the NLC matrix. Let us use the method proposed in Ref. [9] to evaluate the critica1 value c_* for the case of finite surface energies W.

Consider an assembly of cylinder-like particles in a nematic with the initially uniform director no. Let vector $\mathbf{r}_p$ denote the position of the center of mass for the p-th particle and unit vector $\mathbf{u}_p$–its symmetry axis direction. As formerly, we assume that the deviations of the particle orientation from its equilibrium direction are small: $|\delta\mathbf{u}| \ll 1$. With allowance for Eqs. (9) and (17) the volume distortions of the director field may be presented in the form

$$\delta\mathbf{n}(\mathbf{r}) = \sum_p \frac{qL}{|\mathbf{r}-\mathbf{r}_p|}[\delta_u\mathbf{s} + \delta_n\mathbf{s}]_p \ , \qquad (21)$$

where the term in square brackets is the sum of partial variations of the vector $\boldsymbol{s}$ from Eq. (9) with regard to $\mathbf{u}$ and $\mathbf{n}_0$, respectively, taken at the point $\mathbf{r}_p$. The meaning of such a form of the right-hand side of Eq. (21) becomes clear if to write it explicitly for the cases of parallel and perpendicular orientations of the particles. As it has been shown in Sec.III, at $q > 0$ the equilibrium state is $\mathbf{u}_0 \,||\, \mathbf{n}_0$. Taking the corresponding variations of s, we get

$$\delta_s\mathbf{s} = \mathbf{u}_\perp \ , \quad \delta_n\mathbf{s} = -\delta\mathbf{n} \ ;$$

both functions are defined at the point $\mathbf{r}_p$. Substitution to Eq. (21) yielcls

$$\delta\mathbf{n}(\mathbf{r}) = \sum_p \frac{qL}{|\mathbf{r}-\mathbf{r}_p|}[\mathbf{u}_\perp - \delta\mathbf{n}]_p \ , \qquad (22)$$

and grants that a grain positioned in $\mathbf{r}_p$ causes no distortions if it aligns with the local direction of $\mathbf{n} = \mathbf{n}_0 + \delta\mathbf{n}(\mathbf{r}_p)$.

For the case $\mathbf{u} \perp \mathbf{n}_0$ when the parameter q is negative, the pertinent variations give

$$\delta\mathbf{s} = \mathbf{u}_0(\mathbf{n}_0\mathbf{u}), \quad \delta_n\mathbf{s} = \mathbf{u}_0(\mathbf{u}_0\delta\mathbf{n}).$$

With the use of these formulas, Eq. (21) transforms into

$$\delta\mathbf{n}(\mathbf{r}) = \sum_p \frac{qL}{|\mathbf{r}-\mathbf{r}_p|}[(\mathbf{n}_0\mathbf{u}) + (\mathbf{u}_0\delta\mathbf{n})]_p \ . \qquad (23)$$

Here the right-hand side term, proportional to $\delta\mathbf{n}$, as well as that in Eq. (22), eliminates the long-range distortions when the director field in the point $\mathbf{r}_p$ exactly fits the particle orientation u. However, due to a more complicated relation between $\mathbf{n}_0$ and $\mathbf{u}_0$, the form of

expression inside the bracket in Eq. (23) is less obvious than that of Eq. (22).

To pass to the continuum description, let us act upon Eq. (21) with the spatial Laplace operator ∇^2. With the aid of the relation $\nabla^2(\mathbf{r}-\mathbf{r}_p)^{-1} = -4\pi\delta(\mathbf{r}-\mathbf{r}_p)$, with $\delta(\mathbf{r}-\mathbf{r}_p)$ being the Dirac's delta, this yields the equation

$$\nabla^2\delta\mathbf{n} = -4\pi cqL(\delta_u\mathbf{s} + \delta_n\mathbf{s}) , \qquad (24)$$

where c is the number concentration of the particles.

Using the above-obtained expressions for Ss one gets from Eq. (24) in the considered particular cases

$$\nabla^2\delta\mathbf{n} = -\xi^2(\mathbf{u}_\perp - \delta\mathbf{n}), \quad \text{for } \mathbf{n}_0 \parallel \mathbf{u}_0$$

$$\nabla^2(\mathbf{u}_0\delta\mathbf{n}) = -\xi^2[(\mathbf{n}_0\delta\mathbf{u}) + (\mathbf{u}_0\delta\mathbf{n})], \quad \text{for } \mathbf{n}_0 \perp \mathbf{u}_0$$

where

$$\xi^2 = 4\pi c|q|L . \qquad (25)$$

Both equations have the same formal solution

$$\Phi(\mathbf{r}) = c|q|L \int d\mathbf{r}' \frac{\exp(-\xi|\mathbf{r}-\mathbf{r}'|)}{|\mathbf{r}-\mathbf{r}'|}\psi(\mathbf{r}') , \qquad (26)$$

with $\Phi = \delta\mathbf{n}$ and $\psi = \mathbf{u}_\perp$ for the parallel case, and $\Phi = (\mathbf{u}_0\delta\mathbf{n})$ and $\Psi = -(\mathbf{n}_0\delta\mathbf{u})$ for the perpendicular one. The structure of the kernel in Eq. (26) shows that a distortion arisen by an individual particle is screened out (due to the presence of the other particles) at distances greater than ξ^{-1}. Setting c $\sim 10^{10}$ cm^{-3} and taking q ~ 0.1 (sof achoring) one finds $\xi^{-1} \sim 10$ μm as the reference value.

Assume that inside some region (its size denoted as D) of the FN sample a unison rotation Su $\neq 0$ of the particles imposed, while elsewhere Su = Q In this case the estimation of the integral of Eq. (26) for the points inside the region of rotation gives

$$\Phi \sim [1 - \exp(-\xi D)]\Psi , \qquad (27)$$

which proves that the degree of orientation imposed by the particles on the director field, is determined by the ratio of the specimen size to the screening length ξ^{-1}. For D $\gg \xi^{-1}$ the director distortions are substantial ($|\delta\mathbf{n}| \approx |\delta\mathbf{u}|$), i.e., the particles govern the macroscopic texture of the nematic. In the opposite case D $\ll \xi^{-1}$ the particle- induced director perturbations are minor ($|\delta\mathbf{n}| \ll |\delta\mathbf{u}|$) and, therefore, macroscopically negligible.

As Eqs. (25)-(27) shows, to achieve the collective response, the particle concentration at given D must exceed the critica1 value

$$C_* \sim (|q|LD^2)^{-1} . \qquad (28)$$

In the rigid anchoring limit (q = 1) this estimate coincides with that of Ref. [9]: c, $\sim (LD^2)^{-1}$. For the finite anchoring c, becomes q^{-1} times larger due to the renormalization of the distortion amplitude: L $\rightarrow |q|L$. The measurements of the critical concentration of the collective behavior c, carried out for lyotropic FN in Refs. [5, 26], had confirmed the scale dependences c, $\propto (LD^2)^{-1}$ of formula (28).

The critical concentration c, may be obtained as well on the basis of very simple estimates. Let us compare the energies associated with two possible modes of response of the NLC matrix to a unison rotation of the particles. The first mode is the individual behavior, when each particle distorts the matrix independently on the others. The energy increment, according to the formula (12) is $\sim \omega KL$ per particle. For a unit volume containing c particles, it is $E_{\text{ind}} \sim c\omega KL$. The second mode, which is the collective response, takes place when the particles are oriented relatively to the director at nearly the equilibrium angle, and the director distortions are smeared over the largest spatial scale available, i.e., the specimen size D. For this case the orientational-elastic contribution to the energy density is $E_{\text{coll}} \sim K|\Delta_\mathbf{n}|^2 \sim K/D^2$. Apparently, the actual mode of response would be the one with the lower energy. Comparison of E_{ind} and E_{coll} shows that the collective mode is favored as soon as

$$c \geq 1/\omega LD^2 .$$

Recalling that the "interfacial" parameter q by the order of magnitude equals to w–see formula (17)–one immediately recovers the relation (28).

If to measure the particle concentration in the units of the dimensionless volume fraction f = cv, where v

is the particle volume, then for the assembly of cylindrical particles one gets with the aid of Eqs. (17) and (28) the lower bound of the collective behavior in the form $f_* = c_* v \sim (Rb/D^2)$. Taking for estimates a thermotropic FN sample (layer) with D $\sim$ 100 pm, R E 35 nm and b $\sim$ 100 nm, we find $f_* \leq 10^{-6}$. This ensures that the amount of the ferromagnetic admixture sufficient to acquire control over the NLC texture, is rather small.

V. Magnetization states of ferronematics

Magnetic properties of FN are the "sum" of contributions from the nematic matrix and ferroparticles. The nematic itself is subjected to the well-known diamagnetic interaction[2] with the external field. This contribution at f $\ll$ 1 does not depend upon the presente of the particles, and further on would be treated as usual. To clarify the origin of the additional terms, one has to consider the orientation of the particles. Each single-domain prolate grain made of a ferromagnetic material with the saturation magnetization I, possesses the permanent magnetic moment $\mu = I_s v \mathbf{u}$, where u denotes the unit vector of the particle major axis. According to relations (19), in a uniform nematic with the director $\mathbf{n}_0$ such particles settle either along (at a < a,) or transversely (at a > a,) to the optical axis of the matrix. Therefore, in the first case the magnetic moments with equal probability acquire directions $\mathbf{n}_0$ or $-\mathbf{n}_0$, in the secon:d casc are oriented in an arbitrary way in the planes normal to no. In other words, depending upon the boundary angle α, the nematic environment (the NLC matrix) creates for the particles the anisotropy either of the "easy-axis" or "easy-plane" type.

In the absence of the external field or without special preparations these systems are exgected to stay in a magnetically compensated state, where their magnetization $\mathbf{M} = (1/\Delta V)\Sigma\mu_i$ i.e., the sum of magnetic moments averaged over a macroscopically f infinitesimal volume element AV, is zero. However, to be able to govern the FN texture, one needs the suspension with a. non-zero initial ("spontaneous") magnetization. For FN whose particles align with the director there exist at least two ways to achieve such a state–see Ref. [9]. Namely, they are:

- the system is cooled from the isotropic phase down to the nematic one in the presence of a uniform magnetic field H parallel to the would-be optical axis of the nematic. (This direction might be determined, for example, by the boundary conditions on the sample walls.) In the isotropic state the particles align their magnetic moments with H, and the temperature-induced transition in the nematic matrix traps this configuration after the removal of the field;
- the already prepared compensated FN sample is subjected to a single short magnetic field pulse with the amplitude H > H,, where H, E $2\pi I_s$ is the particle coercive force. If the duration of the pulse is shorter than the characteristic time of the particle mechanical rotation, then, due to the intraparticle flip of the magnetic moments over the potential barrier of magnetic anisotropy, all the magnetic moments of the particles in a suspension align along the same direction. After this tuning up, the magnetization of FN is fixed by the orientational coupling ($\pi q K L \gg k_B T$). The effective internal field, stabilizing this "spontaneous" magnetization, is H, $\sim \pi q K L / I_s v = 4Kq/I_s d^2$. For $q = 0.1$, I' $= 5 \cdot 10^{-7}$dyn ,I_s = 500G and R = 35nm the estimate yields H, $\sim$ 10 Oe.

Now let us consider a ferronematic with rod-like particles lying in the planes perpendicular to the axis of the nematic. In this situation the previous estimate for the strength H, of the stabilizing field holds as well. But due to the different kind of its symmetry, H, whatever perfectly suppressing the deviations of the particles from the singled-out plane, cannot build up a magnetized state. To create and maintain a non-zero magnetiza- tion, such a system should be subjected to a certain uniformfield H $\perp \mathbf{n}_0$. Rotation of ferroparticles to the direction of $\mathbf{H}_b$ does not distort the equilibrium texture of the nematic matrix, and FN magnetizes like a two-dimensional isotropic paramagnet:

$$M = I_s f I_1(\rho)/I_0(\rho) \, . \qquad (29)$$

Here f is the local value of the solid phase volume fraction, I_1 and I_0 are the modified Bessel functions of the so-called Langevin parameter $\rho = I_s v H_b / k_B T$, which is the ratio of the magnetic energy of the particle to the energy of its thermal motion. The asymptotics of formula (29) are

$$M = I_s f \begin{cases} \rho/2 & \text{for } \rho \ll 1, \\ 1 - 1/2\rho, & \text{for } \rho \gg 1, \end{cases}$$

whence the saturation behavior $\mathbf{M} \to \mathbf{I_s f}$ at $p \gg 1$ is obvious. Using the cited above dimensional data, one finds that $\rho \geq 10$ at room temperature for the field strength as small as $H \leq 1$ Oe. Hence, even a weak field, lying in the "easy plane", makes FN to be magnetized nearly perfectly.

Since further on we shall deal only with the magnetized FN it is convenient to describe their macroscopic magnetization distribution by a unit vector $\mathbf{m}(\mathbf{r})$ defined by relation

$$\mathbf{M} = I_s f \mathbf{m}(\mathbf{r}) , \qquad (30)$$

where the averaging over the volume element $\Delta V \gg L^3$ is implied. Adopting relation (30), we take for granted that FN is locally saturated. For rigid anchoring, as in Ref. [9], formula (30) immediately reduces to $\mathbf{M} = I_s f \mathbf{n}$. For the case of soft anchoring, Eq. (30) should be taken in its initial form. One has just to remember that in this case the basic state of FN is not completely field-free, but includes a certain small uniform bias field $\mathbf{H}_b$ fixing the direction of m inside the "easy plane". In any applied field H, the resulting distribution $\mathbf{m}(\mathbf{r})$ is determined by the joint action of $\mathbf{H} + \mathbf{H}_b$. As it has been already shown, the reference value of H_b is tiny; in the experiments of Refs. [15, 16, 17, 18, 19] as such the terrestrial magnetic field (~ 0.5 Oe) had been employed.

VI. Free energy of a ferronematic

To solve any macroscopic problems concerning ferronematics, one needs to have the pertinent free energy expression. The corresponding formula for the soft-anchoring case follows from the above presented considerations. First we write it dow

$$\begin{aligned} F &= 1/2[K_1(\mathrm{div}\mathbf{n})^2 + K_2(\mathbf{n} \cdot \mathrm{curl}\mathbf{n})^2 + K_3(\mathbf{n} \times \mathrm{curl}\mathbf{n})^2] - 1/2\chi_a(\mathbf{nH})^2 \\ &- I_s f(\mathbf{mH}) + (f k_B T/v) \ln f + (AWf/2R)(\mathbf{nm})^2 , \end{aligned} \qquad (31)$$

and then explain its structure. The first bracket represents the conventional Frank potential of the nematic matrix, K_i (i = 1, 2, 3) being the orientation-elastic moduli. The second term is also standard, and yields the density of the magnetic energy of the nematic matrix. There χ_a stands for the anisotropic part of the NIC diamagnetic susceptibility; for all usual nematics χ_a is positive. The next two terms of Eq. (31) are the magnetic energy of ferroparticles in the externa1 field, transformed using Eq. (30), and the contribution of the mixing entropy of the their ideal solution, respectively. The last term of Eq. (31) is more peculiar and needs clarification. Returning to Eq. (20) for the energy of the individual particle in the soft-anchoring limit, we may rewrite its part depending on the particle orientation as

$$\mathcal{F}(\theta) = (AWv/2R)(\mathbf{un}_0)^2 , \qquad (32)$$

where parameter $A = -2P_2(\cos\alpha)$ – see Eqs. (17)-(20)–is determined by the boundary conditions. We assume that for an orientationally-deformed magnetized FN this equation holds as well if to replace $\mathbf{u} \to \mathrm{m}$ and $\mathbf{n}_0 \to \mathrm{n}$. . Proceeding to the macroscopic scale and multiplying Eq. (32) by the particle concentration c, one recovers the particle-matrix interaction term entering Eq. (31). For homeotropic orientation we have $\alpha = \pi/2$ – see Fig.1, and thus $A = 1$.

The proposed continuum expression (31) is specified to describe FN with weak ($w < 1$) orientational coupling. According to it, the state of FN is characterized by three thermodynamically-independent spatial distributions: director $\mathbf{n}(\mathbf{r})$, particle concentration $f(\mathrm{r})$ and unit vector of magnetization $\mathbf{m}(\mathbf{r})$. It is worth to remind that the model of Ref. [9], that takes for granted the rigid anchoring of NLC on the particles, prescribes the unbreakable relation $\mathbf{m}(\mathbf{r}) = \mathbf{n}(\mathbf{r})$, thus eliminating $\mathbf{m}(\mathbf{r})$ from consideration. Note, however, that the same result follows as well from Eq. (31) after the limiting transition $\mathrm{W} \to \infty$ at $\mathrm{A} < 0$.

VII. Bonding equation and seggregation effect in a ferronematic

Integrating the energy density (31) over the volume of the FN sample, we get the total free energy in the form of a functional $\tilde{F} = \int F dv$. Its minirnization with respect to $\mathbf{m}(\mathbf{r})$ yields the equation for the equilibrium magnetization

$$(\mathrm{m} \times \mathrm{H},) = 0 , \tag{33}$$

where the effective field governing the orientation of magnetic particles in FN is

$$\mathrm{H}, = -\delta\tilde{\mathrm{F}}/\mu\delta\mathbf{m} = \mathrm{H} + H_a(\mathbf{mn})\mathbf{n}, \mathrm{H}, = -AW/I_aR . \tag{34}$$

These formulas show that the spatial distribiition of the magnetization direction $\mathbf{m}(\mathbf{r})$ depends upon both the external field H and the internal, parallel to the director, anisotropy field H,. In the equilibrium state the vector triad $\mathbf{H}, \mathbf{m}$, and n should be coplanar in each point of the sample. At given H , Eq. (33) with allowance for Eq. (34) couples the orientational distributions $\mathbf{m}(\mathbf{r})$ and $\mathbf{n}(\mathbf{r})$ thus modifying the rigid anchoring model. With regard to this fact, further on we shall refer to Eq. (33) as the bonding equation. In scalar representation it reads

$$\mathrm{H}, \sin 2\theta = 2\mathrm{H}\sin(\chi - \theta) ,$$

where the angles are defined in Fig.2.

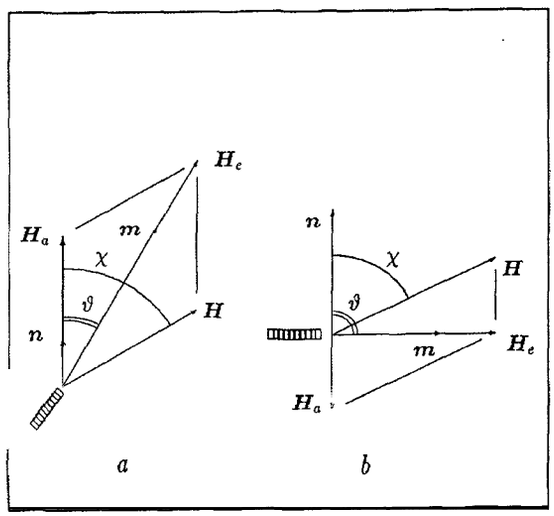

Figure 2: On the definition of the effective rnagnetic field acting on the rnagnetization of FN for the cases of positive (a) and negative *(b)* anisotropy. Note that the dashed rod is drawn only as an eye guide, all the presented vectors are the variables of the macroscopic model.

Note that Eqs. (33)-(34) closely resemble (in fact, coincide with) those describing the equilibrium orientation of the magnetic mornent in a single-domain ferromagnetic crystal with a uniaxial anisotropy (see Ref. [27], for example). In the latter case the orientation-dependent part of the particle energy is

$$U = -I_s v(\mathbf{mH}) - K_a v(\mathbf{m}\nu)^2 ,$$

where K_a is the magnetic anisotropy constant and v is the unit vector of the magnetic anisotropy axis direction. If to fix the particle orientation, i.e., vector v, then the equilibrium direction of the magnetic moment m is determined by minimization of U with respect to m . This yields exactly Eqs. (33) and (34) where now $\mathrm{H}, = 2K_a/I_s$. That means that in FN the nematic matrix is the source of a uniaxial anisotropy field acting on the ferroparticles, $-AW/2R$ being the anisotropy constant. This effective field singles out the preferable directions and stabilizes the remanence magnetization of FN. As far as the external field is weak ($\mathrm{H} \ll |H_a|$) ferroparticle orientation is governed by the director. Since in real FN the amplitude H, is about 100e, it means that the particle coupling with the NLC matrix might be considered as "rigid" only if $\mathrm{H} \lesssim 1$ Oe. In the opposite limiting case ($\mathrm{H} \gg |H_a|$), i.e., $\mathrm{H} \geq 10^2$ Oe, the particle orientation is controlled by the applied field.

Now let us evaluate the equilibrium distribution of the particle concentration. Minimization of the functional $\tilde{\mathcal{F}}$ with respect to $f(\mathbf{r})$ gives the Botzmann-Iike formula

$$f = f_0 \exp\left[\frac{I_s v}{k_B T}(\mathbf{mH}) - \frac{AWv}{2k_B TR}(\mathbf{nm})^2\right] , \quad (35)$$

where the constant f_0 is determined by the usual normalizing condition

$$\int_V f(\mathbf{r})dV = N ,$$

fixing the total number N of the particles.

At H = 0 vector m according to Eqs. (33)-(34)is always parallel to the anisotropy field, that means (nm) = const(r). This makes Eq. (35) trivial, so that it does not affect any initial distribution of concentration. Formula (35) becomes important if it is necessary to analyze the field-induced distribution of the particles in an orientationally deformed FN. Consider a uniform magnetic field H imposed on a non-uniformly oriented sample of FN, where the initial concentration of the particles had been constant. Due to the spatial dependence of the orientational texture $\mathbf{n}(\mathbf{r})$, the power exponent in formula (35) becomes a function of coordinates. It increases in those regions of the sample where the particles, being in the most favorable orientation relatively to the local director $\mathbf{n}(\mathbf{r})$ are at the same time most closely aligned with the applied field. Since the distribution (35) is the equilibrium one, we conclude that upon application of the field, the particles move, populating some particular places of the sample, singled out by relative orientation of n and H. This equilibrium concentration re-distribution, that, after Ref. [9], is called the seggregation *effect*, is one of the most remarkable features of FN. Note that it is provoked by a uniform field and has nothing to do with the plain magnetophoresis.

VIII. Diamagnetic Fredericksz transition in a strong bias field

The expression for the free-energy density for FN with w < 1 and any type of boundary condition, derived in Sec. VI, reads

$$\begin{aligned} F &= 1/2[K_1(\mathrm{div}\mathbf{n})^2 + K_2(\mathbf{n}\cdot\mathrm{curl}\mathbf{n})^2 + K_3(\mathbf{n}\times\mathrm{curl}\mathbf{n})^2] - 1/2\chi_a(\mathbf{nH})^2 \\ &- I_s f(\mathbf{mH}) + (fk_B T/v)\ln f + (AWf/2R)(\mathbf{nm})^2 , \end{aligned} \quad (36)$$

Here χ_a is the anisotropic part of the diamagnetic susceptibility of nematic, H is the externa1 field, M_s, is the saturation magnetization of the particle substance, R and v are the radius of a rod-like particle and its volume, respectively, m is the unit vector of the FN magnetization direction defined as $\boldsymbol{M} = I_s$f m and $\boldsymbol{f}$ is the volume fraction of the particles. Coefficient $A = 1 - 3\cos^2 a$ characterizes the type of the boundary condition, where a is the easy-orientation angle for of the nematic director n on the particle surface; for homeotropic anchoring A is positive and equals to unity.

In the following we apply our model to the orientational behavior of FN with the homeotropic soft ($A = 1, \omega < 1$) anchoring and use the results to interpret the experimental data on real thermotropic FN reported in a series of papers[15,17,18]. While considering the FN layers, we take for granted that in the initial unperturbed state the sample (i) consists of a single liquid-crystalline domain and (ii) is subjected to a permanent bias field $\mathbf{H}_b \perp \mathbf{n}_0$ due to which is magnetized up to saturation with $\mathbf{M}_0 = I_s f\mathbf{m}_0$ along the direction of $\mathbf{H}_b$. The first of these assumptions is a usual idealization to avoid taking into account the liquid-crystalline defects of non-magnetic origin. The second one, as it is shown in Sec. V, is necessary both in theory and experiment to remove the orientational degeneracy of the particle magnetic moments which occurs in the "easy-plane" structures where $\mathbf{M}_0$ is perpendicular to ***no.*** In the above-used notations, as well as in below, the subscript 0 refers to the orientational variables describing the initial state of the sample which is supposed to be spatially uniform.

We begin with the re-consideration of the classical liquid-crystalline effect–the Fredericksz transition–

caused by the diamagnetic anisotropy of the nematic mclecules. The initial geometric patterns of the considered FN cells are presented in Fig.3. Each cell is taken to be an infinite flat layer with the thickness D bounded by solid plane walls where either planar or homeotropic boundary conditions are imposed on the nematic. The diamagnetic susceptibility anisotropy of the latter is supposed to be positive: $\chi_a > 0$.

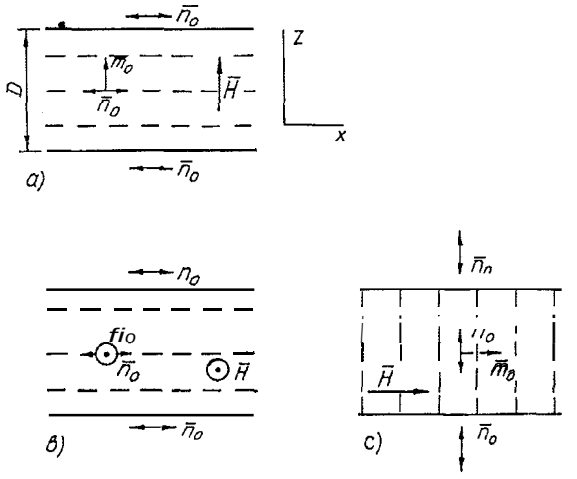

Figure **3:** Initial textures of the FN cells with planar (a and b) and homeotropic (c) anchoring, where the diamagnetic Fredericksz transition takes place.

If to look at any pattern in Fig. 3, it is clear that the bias field $\mathbf{H}_b$, while increasing, plays an ambiguous role: it stabilizes the magnetic particles alignment since $\mathbf{H}_b \,||\, \mathbf{m}_0$, and decreases the stability of the nematic matrix orientation since $\mathbf{H}_b \perp$ no. For a pure nematic (no ferroparticle dope) the eventual result of H_b growth is well-known: immediately after overcoming the threshold H, $\simeq (\pi/D)(K/\chi_a)^{1/2}$ the uniformity of the initial texture breaks down. This phenomenon, called *the* Fredericksz transition, is inherent to anisotropic fluids, and has many modifications in magnetic as well as electric fields–see Ref. [2], for example.

From Eq. (36) it follows that in FN the destabilizing diamagnetic term $\sim \chi_a(\mathbf{nH})^2$ is counteracted by the stabilizing "ferromagnetic" one $\sim \mathbf{I, f(mH)}$. We remind that in the initial geometry $\mathbf{r}_0 \perp$ mo. It is clear that in the long run the diamagnetic contribution, being proportional to H^2, prevails. However, the presence of ferroparticles must shift the value of the critica1 field-strength of the Fredericksz transition upward.

For quantitative results, let us focus on the cell slretched in Fig.3a. In the initial (non-perturbed) state the FN specimen magnetization $\mathbf{M}_0 = I_s \bar{f} \mathbf{m}_0$, where $\bar{f}$ is the average volume fraction of the particles. We set the z-axis of the coordinate framework along the $\mathbf{H}_b$ direction and consider the stability of the initial pattern against the perturbations ofn, m and f. Assuming that they depend only upon the z-coordinate, with linear accuracy one has

$$\begin{aligned} n &= (1, n_y(z), n_z(z)), \\ \mathbf{m} &= (m_x(z), m_y(z), 1), \\ f &= \bar{f} + \delta f \,, \end{aligned} \tag{37}$$

where n_y, n_z, m,, m_y and $\delta f/\bar{f}$ are small comparing to unity. For a translationally uniform in the x-direction case the integration of the function $\mathbf{F}$, given by Eq. (36), across the layer yields the functional $\mathcal{F}$ that is the free-energy density of the system per unit area of the wall. Expanding this functional into a power series in perturbations (37), up to the lowest nonvanishing order, one gets the expression for the free energy increment in the form [28]

$$\begin{aligned} \delta\mathcal{F} &= 1/2 \int_0^D dz \left[K_1 \left(\frac{\partial n_z}{\partial z}\right)^2 + K_2 \left(\frac{\partial n_y}{\partial z}\right)^2 \right. \\ &+ \left. \frac{k_B T}{v} \frac{(\delta f)^2}{f} + \frac{\bar{f} W}{R}(m_x + n_z)^2 + I_s \bar{f} H (m_x^2 + m_y^2) - \chi_a H^2 n_z^2 \right] \end{aligned} \tag{38}$$

Here we have temporarily omitted the subscript b at the bias field H_b.

As it follows from Eq. (38), the pcrturbations n_y, m_y and δf do not interact, and thus do not contribute to the destabilizing effect. Due to that, they might by omitted. In the functional space n, $(z) \otimes m_x(z)$

the line of the steepest descent to the stability threshold 6 3 = 0 is the way along which the functional is minimum with respect to either of its variables. Let us take $m_x(z)$ as the independent one. Then the equation for the extremum trajectory is given by condition $\delta\mathcal{F}/\delta m_x = \Omega$ The explicit form of the latter,

$$m_x = -n_z(1 + I_s HR/W)^{-1} , \qquad (39)$$

yields the relationship between the most dangerous perturbations. Substitution of Eq. (39) into Eq. (38) eliminates m_x and gives

$$\delta\mathcal{F} = 1/2 \int_0^D dz \left[K_1 \left(\frac{\partial n_z}{\partial z} \right)^2 + \left(\frac{W\bar{f} I_s H}{W + I_s HR} - \chi_a H^2 \right) n_z^2 \right] . \qquad (40)$$

Now we need to specify the boundary conditions on the cell walls. It is worth reminding that even for the finite boundary energy the anchoring of n might be treated as rigid, if to consider imaginary walls shifted beyond the real ones by the extrapolation length b. In our case b = K/W ranges from 0.5 to 5 μm. Since we intend to deal with the FN cells not thinner than D $\sim$ 100 pm, the smallness $b \ll$ D enables us to neglect the non-rigidity on the cell walls and set the director perturbations there equal to zero. Taking advantage of this simplification, we expand n, into the Fourier series

$$n_z = \sum_{l=1}^{\infty} \nu_l \sin(\pi l z/D) ,$$

$$n_z(0) = n_z(D) = 0 .$$

Substituting this into Eq. (40) and performing the integration, we get the energy increment in the form

$$\delta\mathcal{F} = (D/4) \sum_l \left[K_1 \left(\frac{\pi l}{D} \right)^2 - \chi_a H^2 + \frac{W\bar{f} I_s H}{W + I_s HR} \right] \nu_l^2 ,$$

where the expansion amplitudes (square brackets) are diminishing functions of the field strength. Setting the smallest of them equal to zero, i.e., focusing on the utmost large-scaled perturbation mode ($l = 1$), we arrive at equation

$$\tilde{H}_c^2 = H_c^2 + G^2(\tilde{H}_c) ,$$

$$G(H) \equiv \left[\frac{W\bar{f} I_s H}{\chi_a (W + I_s HR)} \right]^{1/2} , \qquad (41)$$

determining the Fredericksz transition threshold $\tilde{H}_c$ in FN; here H, = $(\pi/D)(K_1/\chi_a)^{1/2}$ is the critical field value in a pure nematic.

Solution of Eq. (41) is easy, because at H $\sim 10^2$ Oe there exists the small parameter W/I_sHR $\ll 1$; in the first order in it, Eq. (41) transforms into

$$\tilde{H}_c^2 = H_c^2 + G^2 , \quad G = G(\infty) = (W\bar{f}/\chi_a R)^{1/2} , \qquad (42)$$

thus proving the expected increase of the instability threshold. So we see that in the geometries of Figs.3 a-c, the applied field stabilizes the particle orientations, and thus effectively counteracts the approaching instability. Calculations show that formulas (41)- (42) hold for each cell in Fig.3, except that for the pattern b the elastic modulus K_1 in H, must be replaced by K2 (twist) and for c - by K_3 (bend).

Let us estimate the range of the particle-induced contributions to $\tilde{H}_c$ in the thermotropic FN. Setting $\chi_a \sim 10^{-7}$ W $\sim 10^{-2}$ dyn/cm and substituting $\bar{f} \sim 10^{-6}$ and R $\approx$ 35nm, one gets G $\sim$ 150 Oe. This prediction is in qualitative agreement with the observatioris of Ref. [15]–the only one that had dealt with the herein considered geometries. Though no regular quantitative data are reported, the fact that at D $\sim$ 300 pm the orientational transition takes place only at H > 200 Oe is clearly stated there.

IX. Magnetic field-induced birefringence

IX.1 Formula for the optical phase lag

In the preceding Section we have given an example, how the presence of magnetic particles modifies the classical liquid-crystalline effect in FN. Hereafter we address the phenomena of another type–the field-induced effects which are exclusively inherent to ferronematics and are provoked by magnetic fields whose order of magnitude does not exceed 10 Oe. Apparently, in these low fields the diamagnetic term in Eq. (36) is by all means insignificant and hence may be omitted.

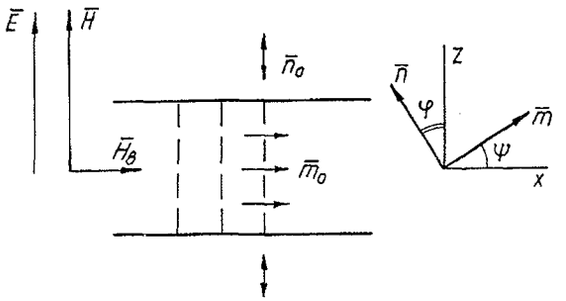

Figure 4: A flat layer of a ferronematic in the external magnetic field H, $= \mathrm{H} + \mathbf{H}_b$; in the right-hand part the choice of the coordinate axes and reference angles is shown. The electric field E is present only for the case considered in Sec.X.

Consider a magneto-optical effect in the orientational structure presented in Fig.4. Homeotropic FN cell is subjected to a constant external field having two components: H and $\mathbf{H}_b$, respectively, parallel and normal to the unperturbed director $\mathbf{n}_0$. According to the concept of magnetization of FN with soft anchoring, proposed in Sec.V, we assume that small bias field $H_b \sim 1$ Oe is imposed and fixed once and forever, while the value of H may change arbitrarily. In the initial state, that is $\mathrm{H} = 0$, the ferromagnetic admixture is homogeneously distributed over the cell volume and the sample is uniformly magnetized up to the saturation value $M_0 = \mathbf{I}_s \bar{f}$ in the direction of $\mathbf{H}_b$. Distortions induced by the field $\mathrm{H} + \mathbf{H}_b$ are characterized by two orientational distributions

$$\begin{aligned} \mathbf{n} &= (-\sin\varphi(z), 0, \cos\varphi(z)), \\ m &= (\cos\psi(z), 0, \sin\psi(z)) \ ; \end{aligned} \qquad (43)$$

the choice of the angles and coordinate axes is shown in the right-hand side of Fig.4. This texture is birefringent for any light beam propagating along the z-axis. The optical phase lag between the extraordinary (refraction index n,) and ordinary (n_0) rays is given by formula

$$\delta = \frac{2\pi}{\lambda_{\mathrm{light}}} \int_{-D/2}^{D/2} (n - n_0) dz \ , \qquad (44)$$

where λ_{light} is the wavelength of the light in the empty space, D is the cell thickness and $\mathrm{n} = n(z)$ is the effective refraction index defined as

$$n^{-2}(\mathrm{z}) = n_0^{-2} \cos^2\varphi(z) + n_e^{-2} \sin^2\varphi(z) \ .$$

Let us derive a set of equations describing the equilibrium state of FN at given H and evaluate the dependente $\delta(H)$. The expression for the free-energy functional $\mathcal{F}$ is obtained by integration of Eq. (36) across the cell, with Eqs. (43) substituted therein. This gives

$$\begin{aligned} \mathcal{F} &= \int_{-D/2}^{D/2} dz \Big[1/2 K_3 \vartheta'^2 (1 + p \sin^2 8) \\ &- \mathbf{I}_s \mathrm{f} (H_b \cos\psi + \mathrm{H} \sin\psi) \\ &+ \frac{fW}{2R} \sin^2(\psi - \vartheta) + \frac{f k_B T}{v} \ln f \Big] \ . \end{aligned} \qquad (45)$$

Here we have introduced a dimensionless parameter $p = (K_1 - -K_3)/K_3$, and use the prime to denote differentiation with respect to z. As it follows from Eq. (45), $\mathcal{F}$ depends upon three functions: angular distributions $\vartheta(z)$ and $\psi(z)$ and concentration f(z); the sought for equilibrium equations are yielded by corresponding variations of $\mathcal{F}$. The first of them $(\delta\mathcal{F}/\delta\vartheta = 0)$ transforms into

$$\begin{aligned} &\vartheta''(1 + p \sin^2 0) + \vartheta'^2 p \sin\vartheta \cos 2\vartheta \\ &+ (fW/2K_3R) \sin 2(\psi - \vartheta) = 0. \end{aligned} \qquad (46)$$

The second $(\delta\mathcal{F}/\delta\psi = 0)$ has the meaning of the bonding equation–see Sec.VII–and takes the form

$$\mathbf{I}_s (H_b \sin\psi - H \cos\psi) + (W/2R) \sin 2(\psi - \vartheta) = 0 \ . \qquad (47)$$

The third one $(\delta\mathcal{F}/\delta\psi = 0)$ accounts for the seggregation effect–see Sec.VI, and reads

$$\begin{aligned} f &= \bar{f} Q \varepsilon(\psi, \varphi) \ , \\ Q &= D \left[\int_{-D/2}^{D/2} \varepsilon(\psi, \vartheta) dz \right]^{-1} \ , \end{aligned} \qquad (48)$$

where

$$\varepsilon(psi, 8) = \exp[\rho_b \cos\psi + \mathrm{p} \sin\psi - \sigma \sin^2(\psi - \vartheta)] \ ;$$

and the scaled by temperature dimensionless parameters are

$$\rho_b = I_s v H_b / k_B T \ ,$$

$$\rho = I_s v H_b / k_B T \ ,$$

$$\sigma = Wv/2k_BTR \ .$$

As the first step to solve the set (46)-(48), we multiply Eq. (46) by ϑ', Eq. (47) by $f\psi'$ and subtract the latter from the former simultaneously substituting f from Eq. (48). In result we arrive at the integro-differential equation

$$K_3\vartheta'[\vartheta''(1+p\sin^2\vartheta)+p\vartheta'^2\sin\vartheta\cos\vartheta]+$$
$$+(\bar{f}QW/2R)\varepsilon(\psi,\vartheta)(\vartheta'-\psi')\sin 2(\psi-\vartheta)+$$
$$+I_s\bar{f}Q\psi'\varepsilon(\psi,\vartheta)(H\cos\psi-H_b\sin\psi)=0 \ . \quad (49)$$

Together with the bonding Eq. (47) it determines, though implicitly, the orientational distributions $\vartheta(z)$ and $\psi(z)$.

As it has been explained in Sec.VIII, for sufficiently thick layers the difference between soft and rigid anchoring of nematic at the cell wall is irrelevant, and we way as well impose rigid boundary conditions on 19. It is natural to anticipate that in the middle plane of the layer the angular deviations are maximum. Thus, for the orientational profile we set

$$\vartheta(\pm D/2)=0 \ , \quad \vartheta'(0)=0 \ . \quad (50)$$

For Eq. (49) the first integra1 is available. Wíth the aid of the second of the conditions (50) it may be written as

$$\lambda^2\vartheta'^2(1+p\sin^2\vartheta)-Q[\varepsilon(\psi_m,\vartheta_m)-\varepsilon(\psi,\vartheta)]=0 \ . \quad (51)$$

Here the angles $\vartheta_m \equiv \vartheta(0)$ and $\psi_m \equiv \psi(0)$, connected by Eq. (47), describe the angular positions of the director and magnetization vector in the middle plane of the cell. The length parameter $\lambda = (K_3v/2\bar{f}k_BT)^{1/2}$ determines the distance by which the orienting influence of the wall penetrates into a semi-infinite FN sample in a sufficiently strong magnetic field[9,10].

Resolving Eq. (51) for dz, one finds

$$dz = \mp\lambda Q^{-1/2}(1+p\sin^2\vartheta)^{1/2}[\varepsilon(\psi_m,\vartheta_m)-\varepsilon(\psi,\vartheta)]^{-1/2}d\vartheta \ ; \quad (52)$$

here the signs $\mp$ refer to the upper and lower half-spaces, respectively–see Fig.4. Integration of Eq. (52) at $z > 0$ with allowance for Eq. (50) yields

$$(D/2-z)/\lambda = 2Q^{-1/2}I(\vartheta) \ , \quad (53)$$

where

$$I(\vartheta)=\int_0^{\vartheta}(1+p\sin^2 y)^{1/2}[\varepsilon(\psi_m,\vartheta_m)-\varepsilon(\psi(y),y)]^{-1/2}dy$$

In the plane $z = 3$, where $\vartheta = \vartheta_M$, Eq. (53) transforms into equality

$$D/\lambda = 2Q^{-1/2}I(\vartheta_m) \ , \quad (54)$$

that enables to eliminate the coefficient Q and rearrange Eq. (53) as

$$1-2z/D = I(\vartheta)/I(\vartheta_m) \ . \quad (55)$$

The last relation and the bonding Eq. (47) that may be rewritten in the form

$$\rho_b\sin\psi - \rho\cos\psi + a\sin 2(\psi-\vartheta)=0 \ , \quad (56)$$

make a closed subset determining the orientational dependentes $\vartheta(z)$ and \$@) at given ϑ_m. Using Eq. (52) to change the variables in Eq. (48), we find

$$Q = I(\vartheta_m)/J(\vartheta_m) \ , \quad (57)$$

where

$$I(\vartheta) = \int_0^{\vartheta}(1+p\sin^2 y)^{1/2}[\varepsilon(\psi(y),y)\varepsilon[\psi_m,\vartheta_m) - \varepsilon(\psi(y),y)]^{-1/2}dy \ .$$

Substitution of Eq. (57) into Eq. (54) gives

$$(D/2\lambda)^2 = I(\vartheta_m)\cdot J(\vartheta_m) \ , \quad (58)$$

that completes the full set of equations comprising now Eqs. (55)-(58).

To compare the theoretical expression with the experimentally observed function $\delta(H)$, we transform Eq. (44) with the aid of Eqs. (52) and Eq. (55), thus arriving at the formula

$$\delta = \frac{2\pi n_0 D}{\lambda_{\rm light} I(\vartheta_m)} \int_0^{\vartheta_m} \left[n_e (n_e^2 \cos^2 y + n_0^2 \sin^2 y)^{-1/2} - 1 \right] (1 + p \sin^2 y)^{1/2} \times [\varepsilon(\psi_m, \vartheta_m) - \varepsilon(\psi(y), y)]^{-1/2} dy \ , \quad (59)$$

describing the phase lag between the ordinary and extraordinary rays in a deformed by field H texture of FN.

IX.2 Comparison with the experiment

The results of numerical evaluation of the theoretical dependence $\delta^{1/2}(H)$ given by Eq. (59) for a number of cell thicknesses and particle concentrations are presented in Figs. 5 and 6. Various dots are the experimental data reported in Ref. [15] for the birefringence of flat FN cells. The observations were performed at room temperature, the initial orientation patterns corresponded to those sketched in Fig.4. The carrier of FN was the well-known liquid crystal MBBA (methoxybenzylidene butylaniline), whose elastic moduli, according to Ref. [2], are $K_1 \approx 5 \cdot 10^{-7}$ dyn and $K_3 \approx 8 \cdot 10^{-7}$ dyn. The wavelength of the laser light was $\lambda_{\rm light} = 632.8$nm; for the refraction indices of MBBA, after Ref. [29], we set $n_0 \approx 1.5$ and $n_e \approx 1.7$. The role of $\mathbf{H}_b$ in Ref. [15] was played by the terrestrial magnetic field whose strength in our calculations we have set to 0.6 Oe. For the given particle size: length L ≈ 500 nm and diameter 2R ≈ 70nm, this bias field yields $\rho_b \approx 10$. For the amplitude W of the anisotropic part of the anchoring energy (the particles were coated with the DMOAP surfactant–see Ref. [15]) we took $5 \cdot 10^{-2}$ dyn/cm.

The most difficult step in the interpretation is to estimate the particle concentration. Indeed, while FN preparation there occurs a partial coagulatiori of the magnetic grains, i.e., formation of large multi-particle aggregates. Since such an object has a closed configuration of constituting magnetic moments, its net moment is nearly zero. Due to that the aggregates becorne insensitive to the action of weak external fields thus dropping out of the considered birefringence effect. In result, the volume fraction of the particles, which really impart strong magneto-optical properties to FN, must reduce substantially in comparison with the total solid phase content of the suspension. However, a reasonable estimate for the true concentration of single-domain particles may be found from the experimental data plotted in Figs.5,6.

Consider the response of the liquid-crystalline suspension in an extremely weak magnetic field $H < H_b$, i.e., $\rho < \rho_b < \sigma$. In this case Eq. (56) allows to treat the local bonding of the orientational distributions $\mathbf{n}(z)$ and $\mathbf{m}(z)$ as rigid: $\psi(z) = \vartheta(z)$, i.e., $\mathbf{n} \perp \mathbf{m}$ –see Fig.4. Solving the *properly simplified* Eqs. (55) and (58), one finds that at $\rho\vartheta_m \ll 1$ function $\vartheta(z)$ has the parabolic profile

$$\vartheta(z) = (I_s \bar{f} H D^2 / 8K_3)[1 - -4z^2/D^2]$$

Substituting this into the integral (59), for the phase lag in the $\rho\vartheta_m \ll 1$ range, one gets

$$\delta^{1/2}(H) = [\pi D^5 (n_e - -n_0)/60\lambda_{\rm light}]^{1/2} (I_s \bar{f} H / K_3) \ . \quad (60)$$

This expression proves that in weak fields function $\delta^{1/2}$ is linear in the field-strength and its initial slope is directly proportional to the sought for magnetic admixture concentration $\bar{f}$ not yet spoiled by the seggregation effect. In our interpretation we deduce the true value $\bar{f}$ applying formula (60) to the initial regions of the experimental curves. The reference (lowest) concentration $\bar{f}_m$ by which the volume fraction $\bar{f}$ is scaled in Figs. 5 and 6, has been evaluated from the line 2 in Fig.6; the result is $\bar{f}_m = 7 \, . \, 10^{-8}$. Further on, this very value, being about 40% of the total solid phase amount 1.86×10^{-7} reported in Ref. [15], had been used in the fitting procedures for all other theoretical

curves (solid lines) plotted in Figs. 5, 6. We suppose that for two particular experiments, corresponding to curve **3** of Fig.5 and curve **1** of Fig.6, the normalizing factor $\bar{f}_m$ has somehow deviated considerably from the cited value of $\bar{f}_m$. This assumption is confirmed by the results of re-calculation (dashed lines in Figs. 5,6) with the changed values of $\bar{f}$.

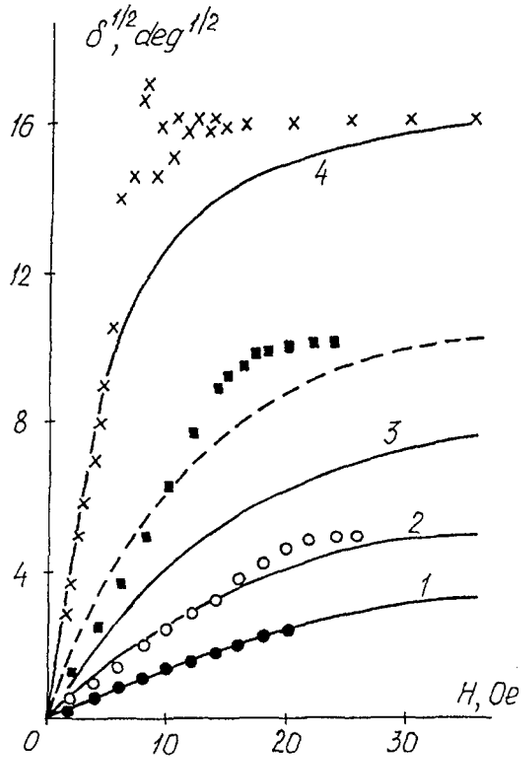

Figure 5: Field-strength dependences of the optical phase lag for different thicknesses D of the FN cell. The assumed initial concentration of single-domain ferroparticles $\bar{f} = 1.12 \cdot 10^{-6}$; the given in Refs. [15,171 total one evaluated by weight measurement is $\bar{f} = 2.98 \cdot 10^{-6}$. Lines–theory, dots–experimental data by Ref. [15]; D = 123 μm (curve 1 and black circles), 152 μm (*2* and empty circles), 189 μm (*3* and squares), 354 pm (4 and crosses). The dashed line (cf. curve 3) is the theoretical curve for D = 189μm at $\bar{f} = 2.0 \cdot 10^{-6}$.

In their general features, the obtained theoretical dependences based on Eq. (59) agree with the experimental data. In weak fields the dots reasonably comply with the linear function (60). Further growth of the birefringence $\delta^{1/2}(H)$ is more slow in comparison with the linear law, and in the H ~ 20 – –40 Oe range both theoretical and experimental graphs show the optical saturation of FN. The observed oscillations of $\delta^{1/2}(H)$ in some curves are most probably, as it has already been mentioned in Ref. [15], caused by the coagulation of ferroparticles. Indeed, in a dilute system coagulation of ferroparticles is the direct result of the seggregation effect. The latter provokes the re-distribution of the particles even in rather weak fields. In particular, at $\rho\vartheta_m \ll 1$ from Eqs. (48) and (57) it follows

$$f(z) = \bar{f}[1 + \rho^2 D^2(1 - -12z^2/D^2)/48\lambda^2] , \qquad (61)$$

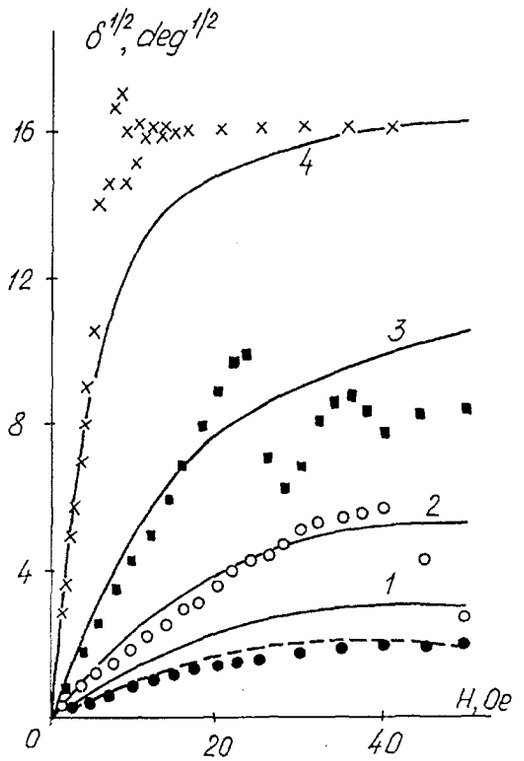

Figure 6: Field-strength dependence of the optical phase lag for different concentrations of single-domain ferroparticles at D = 354μm (curves *1*, *3*, 4) and D = 337μm (curve 2). Lines–theory, dots experimental data by Ref. [17]; f = $\bar{f}_m = 7 \cdot 10^{-8}$ (*1* and black circles), $2\bar{f}_m$ (*2* andempty circles), $4\bar{f}_m$ (*3* and squares), $16\bar{f}_m$ (4 and crosses). The dashed line (cf. curve *1*) is the theoretical curve for $\bar{f} = 5 \cdot 10^{-8}$.

that means that the particles, minimizing their orientational energy, accumulate in the middle of the cell. The numerical calculations show that with H growing, the stratification of the magnetic admixture intensifies. At certain critical concentration the magnetic dipole-dipole interaction must lead to the abrupt local coagulation. Because of that, the fraction of isolated (single) particles reduces, and the observed birefringence falls down. However, the external field continues to grow, increasing the alignment of-the remained grains and,

hence, the induced birefringence of the cell. Simultaneously, seggregation pumps up new portions of particles into the middle section of the cell. Due to that, in this region the concentration grows anew until it once more achieves the critica1 value. Assuming such a sequence of coagulation cycles one gets a reasonable qualitative expla- nation of the observed oscillations of the optical response (see squares and crosses in Figs. 5 and 6).

X. Fredericksz transition in the electric field

X.1 Modification of the transition threshold

Here we study the effect of the bias magnetic field upon the electric Fredericksz transition in a ferronematic. Note that actually it is just this electric instability that is employed in the majority of the liquid-crystalline devices destined for the image processing.

Consider the uniform FN textures presented in Fig.7. We assume that inside the cell there exists a constant bias field $\mathbf{H}_b \perp \mathbf{n}_0$ providing saturated uniform magnetization in the initial state. To take into account the dielectric properties of the liquid-crystalline matrix, one should include into the free-energy density expression (36) the term

$$F_{\text{electr}} = -\frac{\varepsilon_a}{8\pi}(\mathbf{nE})^2 \ . \qquad (62)$$

Bearing in mind a MBBA-based ferronematic, we assume that the dielectric permeability anisotropy ε_a is negative. Then it is natural to expect that the instability of the uniform texture would be provoked by an electric field $E \perp \mathbf{n}_0$. Let us find the Fredericksz transition threshold for the cell with the configuration of Fig.7a. While performing the calculation, we will retain in F the diamagnetic contribution caused by the bias field.

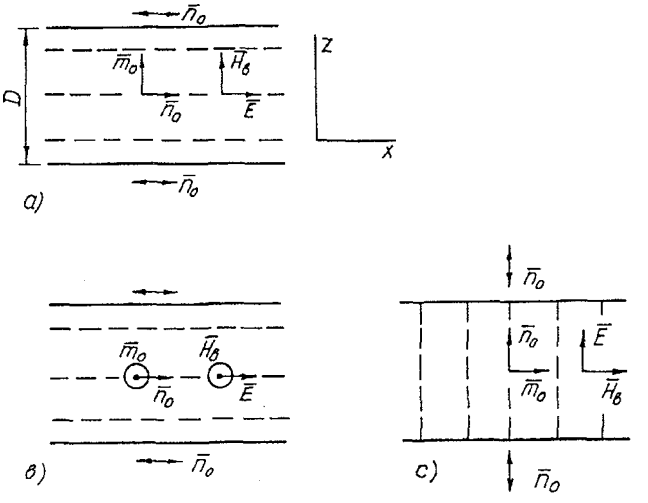

Figure 7: Initial textures of the FN cells with planar (a and b) and homeotropic (c) anchoring, where the diamagnetic Fredericksz transition takes place.

Choosing the orientational perturbations of n and m in the form of Eq. (37), with the accuracy up to the second power in small quantities one finds for the free energy functional

$$\delta\mathcal{F} = 1/2\int_0^D dz\left[K_1\left(\frac{\partial n_z}{\partial z}\right)^2 + K_2\left(\frac{\partial n_y}{\partial z}\right)^2 + \frac{\bar{f}W}{R}(m_x+n_z)^2 + \right.$$
$$\left. + \ I_s\bar{f}H_b(m_x^2 - \chi_a H_b^2 n_z^2 + \gamma_a E^2(n_y^2+n_z^2)\right] \ . \qquad (63)$$

Here we have omitted the terms connected with m_y and Sf which do not contribute to the instability, and introduced the notation $\gamma_a = \varepsilon_a/4\pi$. Evaluating, as in Sec.VII, the line of the steepest descent to the stability threshold by condition $(\delta/\delta m_x)\delta\mathcal{F} = 0$, we arrive at the relation coinciding with Eq. (39) and use it to eliminate m, from Eq. (63). With allowance for the rigid anchoring conditions $\mathbf{n}(0) = \mathbf{n}(D) = \mathbf{n}_0$ on the cell walls, the Fourier transformations

$$n_y = \sum_{k=1}^{\infty}\eta_k \sin\left(\frac{\pi k z}{D}\right)$$

$$n_z = \sum_{k=1}^{\infty}\nu_k \sin\left(\frac{\pi k z}{D}\right)$$

reduce $\delta\mathcal{F}$ to the diagonal form. Integration across the

cell yields:

$$\delta\mathcal{F} = \frac{D}{4}\sum_{k=1}^{\infty}\left\{[K_1\left(\frac{\partial n_z}{\partial z}\right)^2 + K_2\left(\frac{\partial n_y}{\partial z}\right)^2 + \frac{\bar{f}W}{R}(m_x+n_z)^2 + \right.$$
$$\left. + \; I_s\bar{f}H_b(m_x^2 - \chi_a H_b^2 n_z^2 + \gamma_a E^2(n_y^2+n_z^2)]\right. . \qquad (64)$$

where function $G(H_b)$ is defined by formula (41). The calculations for the textures in Figs. 7 b,c give the same result save that for the pattern b moduli K_1 and K_2 in Eq. (64) should interchange their places, and for the pattern c, where the instability is induced by the bend mode, only K_3 instead of K_1 and K_2 enters the expression for $\mathcal{F}$.

In the latter case the stability analysis is most simple. Indeed, for the critica1 electric field from Eq. (64) at $K_i = K_3$ we find the set of equalities

$$\tilde{E}_c = \frac{1}{D|\gamma_a|^{1/2}}\begin{cases}(\pi^2 K_3)^{1/2}\,, \\ (\pi^2 K_3 + \chi_a D\Lambda)^{1/2}\end{cases} \qquad (65)$$

where

$$\mathrm{A} = G^2(H_b) - H_b^2\,,$$

It is apparent, that the observed value $\tilde{E}_c$ of the threshold corresponds to the smaller right-hand side of Eq. (65). That means that we should find out the sign of function $\Lambda(H_b)$. Using Eq. (42), it is easy to show that for $H_b < \mathrm{G} = (\bar{f}W/\chi_a R)^{1/2}$ this quantity is positive, i.e., the bias field stabilizes FN against the perturbations of n,. In this case the Fredericksz transition threshold remains the same as in a pure nematic[2]:

$$\tilde{E}_c = E_c = (\pi/D)(K_3/|\gamma_a|)^{1/2}\,.$$

In the fields $\mathrm{G} < H_b < \mathrm{H}$, the diminution of the critical electric field, accounting for the growth of the destabilizing influence of the magnetic field H_b on the liquid-crystalline the lower line of formula (65).

Now we return to consideration of the electric Fredericksz transition in the texture of Fig.7a. In this case the expressions for the critica1 field-strength read

$$\tilde{E}_c = \frac{1}{D|\gamma_a|^{1/2}}\begin{cases}(\pi^2 K_2)^{1/2}\,, \\ (\pi^2 K_1 + \chi_a D\Lambda)^{1/2}\end{cases} \qquad (66)$$

and for a liquid crystal like MBBA or PAA one may set $K_1 \approx 2K_2$ [2]. Deducing the condition under which the bias field diminishes the threshold of the transition in the electric field, we get

$$H_b^2 - G^2(H_b) > (\pi/D)^2(K_1 - K_2)/\chi_a \approx (\pi/D)^2(K_2/\chi_a)\,,$$

With allowance for Eq. (42) this enables to rewrite the interval of H_b, within which the magnetic orientation reduces the threshold $\tilde{E}_c$ in comparison with the classical case, as

$$(\pi/D)^2(K_2/\chi_a) + G^2 < H_b^2 < (\pi/D)^2(K_1/\chi_a) + G^2\,.$$

For the texture of Fig.7b, where the critical field is determined similarly to Eq. (66), save the replacement $K_1 \leftrightarrow K_2$, the calculation shows that inside the whole available magnetic field range the Fredericksz transition threshold is given by expression

$$\tilde{E}_c = \frac{1}{D}\left(\frac{\pi^2 K_2 + \chi_a \Lambda D^2}{|\gamma_a|}\right)^{1/2}$$

X.2 Comparison with the experiment

The results of observation of the Fredericksz effect in thermotropic FN are reported in Ref. [17]. The studied textures corresponded to the one of Fig.7c; the suspension was magnetized by the terrestrial magnetic field. The critical electric potential difference $\tilde{V}_c = \tilde{E}_c D$ between the cell walls was determined optically by the onset of birefringence for the light beam directed along the z-axis. The dependence $\delta(\tilde{V})$ rendering the phase lag between the ordinary and extraordinary rays in the above-threshold range, i.e., for $\tilde{V} = \mathrm{ED} > \tilde{V}_c$, has

been measured. Let us evaluate $\delta(\tilde{V})$ on the basis of tlie given theory, and compare it with the experimental data of Ref. [17].

As it follows from the results of Sec.X.1, in the configuration of Fig.7c at $H_b \sim 1$ Oe < G the critical field-strength $\tilde{E}_c$ coincides (see Eqs. (65)) with that of apure nematic. Apparently, in the electric field E > $\tilde{E}_c$ = E, the minimum of the free-energy of the deformed FN corresponds to the state where the local director n lies in tlie yOz plane. Under such a distortion the magnetic particles retain the initial orientation along $\mathbf{H}_b$ and remain normal to n all over the bulk of the cell. Due to that, the considered deformation of n does not cause any changes of the particle orientation energy, the equilibrium director distributions above the Fredericksz transition are exactly the same in pure nematic and in FN.

In tlie single-constant approximation $K_1 = K_2 = K_3 = K$ the function $\vartheta(z)$ rendering the angular deviations $\mathbf{n}(z)$ from the direction of the initial orientation $\mathbf{n}_0$ for $0 \leq z \leq D/2$ is defined (see Ref. [2]) by equation

$$z = \xi_{\text{electr}} F(\tilde{\vartheta}, \sin\vartheta_m) \ . \qquad (67)$$

Here $\sin\tilde{\vartheta} = \sin\vartheta/\sin\vartheta_m, \xi_{\text{electr}} = (4\pi K_3 E^2/|\varepsilon_a|)^{1/2}$ is the electric coherence length, $F(\tilde{\vartheta}, \tilde{k})$ is the incomplete elliptic integral of the first kind and $\vartheta_m = \vartheta(D/2)$. Using relationship (67) to change the variable in the integral (44), we arrive at the formula

$$\delta = \left(\frac{2\pi n_0 D}{\lambda_{\text{light}}}\right) \frac{1}{F(\pi/2, \sin\vartheta_m)} \int_0^{\vartheta_m} \left[n_e^2(n_e^2\cos^2 y + n_0^2\sin^2 y)^{-1/2} - 1\right] \times (\sin^2\vartheta_m - \sin^2 y)^{-1/2} dy \ , \qquad (68)$$

which yields the value of birefringence at given electric field-strength E or voltage $\tilde{V}$.

In Fig.8 are presented the theoretical and experimental dependences $\delta(\tilde{V})$ corresponding to two Fredericksz transitions–in a pure nematic and in FN. As the experiments show, in thermotropic suspensions $\tilde{\mathrm{E}}$, is smaller than the corresponding value E, in undoped nematics. This effect may be accounted for the existente of large aggregates comprising a great number of particles. Around such objects the macroscopic director distortions must have been formed which serve as the pre-existing nuclei of the orientationally-deformed state thus favoring the diminution of the transition threshold. In Ref. [17] on the basis of the obtained critical field $\tilde{E}_c$ the effective value of K_3 has been deduced as $\tilde{K}_3 = D|\varepsilon_a|\tilde{E}_c^2/4\pi^3$. At E, = −0.5 the found value had turned out to be $\tilde{K}_3 = 6.37.10^{-7}$ dyn, that is approximately 5% lower than the elasticity modulus $K_3 = 6.74.10^{-7}$ dyn for pure MBBA. The carried out calculations of $\delta(\tilde{V})$ curves for the corresponding Frank constants are in good agreement with the observed data both for undoped MBBA and FN.

XI. Birefringence of a ferronematic in the crossed magnetic and electric fields

XI.1 The set of equations

Finally, let us use the accumulated knowledge, to get a theoretical description of the experiments of Refs. [17, 18] on the birefringence of FN subjected to a combination of electric and magnetic fields. The geometry of tlie cell resembles that of Fig.4 save for the fact that now the electric field is imposed along the z-axis. In the initial state FN is a single liquid-crystalline domain ($\mathbf{n}_0$ = const) all over which the magnetization $\mathbf{M}_0 = I_s\bar{f}$ is perpendicular to the director. The external magnetic field H, inducing the particle rotation and, hence, the rearrangement of the orientational texture, creates in the sample a certain preliminary distortion–see Sec. IX. The electric field $\mathbf{E} = (0, 0, \mathrm{E})$ that acts explicitly on the liquid-crystalline matrix, enhances this distortion tending to rotate the director perpendicular to its initial alignment. In the papers[17,18] a family of the experimental dependences $\delta(\tilde{V})$ for the magnetic field range 1-50e had been measured.

Note that in the presence of the magnetic field $\mathbf{H} \perp \mathbf{M}_0$ the equilibrium state of the deformed texture corresponds to the perturbations of n and m lying in the plane xOz–see Fig.4. From the bonding conditions (32) and (33) it follows that vectors $\mathbf{n}, \mathbf{m}$ and $\mathbf{H}_p$ must be coplanar; here H, $= \mathbf{H}_b + \mathbf{H}$ is the resulting magnetic field whose direction is tilted relatively to the vertical axis z.

Writing down the orientational distributions $\mathbf{n}(z)$ and $\mathbf{m}(z)$ in the form (43), we substitute them into Eq. (45) extended by adding the electrical term Eq. (62). The obtained free-energy functional reads:

$$\mathcal{F} = \int_{-D/2}^{D/2} dz \left[\frac{1}{2}K_3\vartheta'^2(1+p\sin^2\vartheta) - I_s f(H_b\cos\psi + H\sin\psi) + \right. \\ \left. + \left(\frac{fW}{2R}\right)\sin^2(\psi-\vartheta) + \left(\frac{fk_BT}{v}\right)\ln f + \frac{|\varepsilon_a|}{8\pi}E^2\cos^2\vartheta\right] . \tag{69}$$

Variation of $\mathcal{F}$ with respect to $6, \psi$ and f yields the set of the equilibrium equations to determine the orientational and concentration distributions $\vartheta(z), \psi(z)$ and f(z) for given values of the electric and magnetic field-strengths. After the transformations similar to those made for Eqs. (46)-(58), we arrive at the closed set of four equations:

$$D/2\lambda = Q^{-1/2}I(\vartheta_m), \tag{70}$$

$$\mathrm{Q} = I(\vartheta_m)/J(\vartheta_m), \tag{71}$$

$$1 - 2z/D = I(\vartheta)/I(\vartheta_m), \tag{72}$$

$$\rho\cos\psi - \rho_b\sin\psi = \sigma\sin 2(\psi-\vartheta). \tag{73}$$

Here the integrals **I** and **J** are defined as follows:

$$I(\vartheta) = \int_0^{\vartheta}(1+p\sin^2 y)^{1/2}\{Q[\varepsilon(\psi_m,\vartheta_m) - \varepsilon(\psi(y),(y)] + \zeta(\sin^2\vartheta_m - \sin^2 y)\}^{-1/2}dy ,$$

$$I(\vartheta) = \int_0^{\vartheta}(1+p\sin^2 y)^{1/2}\varepsilon(\psi(y),y)\{Q[\varepsilon(\psi_m,\vartheta_m) - \varepsilon(\psi(y),(y)] + \zeta(\sin^2\vartheta_m - \sin^2 y)\}^{-1/2}dy ,$$

and the parameter $\zeta = |\varepsilon_a|E^2 v/8\pi\bar{f}k_BT$ is introduced to characterize the strength of the externa1 electric field; for other parameters the notations of Sec. IX hold.

The optical response of the system to the applied fields obtained by substitution of Eq. (72) into the integral (44) takes the form

$$\delta = \left(\frac{2\pi Dn_0}{\lambda_{\text{light}}}\right)\int_0^{\vartheta_m}\left[n_e^2(n_e^2\cos^2 y + n_0^2\sin^2 y)^{-1/2} - 1\right](1+p\sin^2 y)^{1/2}\times \\ + \{Q[\varepsilon(\psi_m,\vartheta_m) - \varepsilon(\psi(y),y)] + \zeta(\sin^2\vartheta_m - \sin^2 y)\}^{-1/2}dy . \tag{74}$$

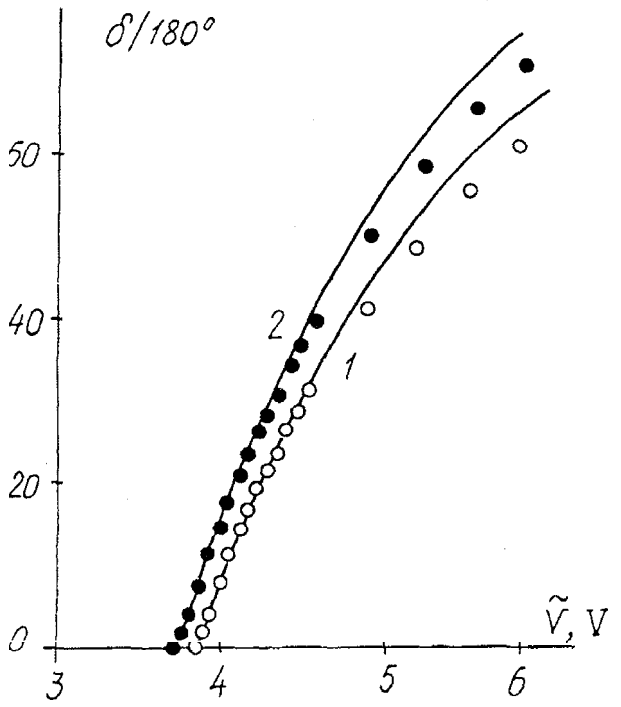

Figure 8: Electric voltage dependence of birefringence above the threshold of the dielectric Fredericksz transition for a pure nematic (curve 1, $D = 222\mu$m $K_3 = 6.74 \cdot 10^{-7}$ dyn) and MBBA-based ferronematic (curve 2, D = 240μm $\tilde{K}_3 = 6.37 \cdot 10^{-7}$ dyn). Lines–calculations by Eq. (68), dots–experimental data by Ref. [17].

XI.2 Orientation and concentration distributions in the ferronematic cell

The initial parts of the theoretical (calculated according to Eq. (74)) and experimental (taken from Ref. [18]) curves $\delta^{1/2}(\tilde{V}^2)$ at H = 1.5, 4.0 and 5.0 Oe are presented in Fig.9; the global view of the dependence $\delta(\tilde{V})$ for H = 2 Oe is shown in Fig.10. The calculations have been carried out by formulas Eq. (70)-(74) in the single-constant approximation with the effective elasticity modulus $K = K_3 = 6.37.\ 10^{-7}$ dyn, as in Ref. [17]. The concentration of single-domain grains $\mathrm{f} = 2.5 \cdot 10^{-7}$ has been determined by comparison of the initial theoretical and experimental values of $\delta(\tilde{V} = \mathrm{O})$. Note that the total solid phase content given in Refs. [17, 18] was $1.89 \cdot 10^{-6}$

Let us firstly consider the FN behavior in weak electric and magnetic fields. Solving Eqs.(70)-(73) under assumptions $\rho\vartheta_m \ll 1$ and $\zeta\vartheta_m^2 \ll 1$, one gets the followingexpressions for the orientation and concentration profiles

$$\vartheta(z) = \frac{M_s \bar{f} H}{8K_3}\left(1 + \frac{|\varepsilon_a|E^2D^2}{32\pi K_3}\right)(D^2 - 4z^2)\ ;$$

$$f(z) = \bar{f}[1 + \rho^2 D^2(1 + \zeta/8\lambda^2)(1 - 12z^2/D^2)/48\lambda^2]\ .$$

Substitution of $\vartheta(z)$ into the integral (74) gives the optical response in the form

$$\delta = \left[\frac{\pi(n_e - n_0)D^5}{60\lambda_{\mathrm{light}}}\right]\left(\frac{M_s \bar{f} H}{K_3}\right)^2\left(1 + \frac{|\varepsilon_a|E^2D^2}{32\pi K_3}\right)^2\ ;$$

duly rescaled, it has been used to describe the initial slopes of $\delta^{1/2}(\tilde{V}^2)$.

As the field-strength grows, the seggregation effect begins to play an important part in formation of the equilibrium texture. With the increase of the magnetic field, the particles gather in the middle section of the cell intensifying the director tilt there. The applied electric field enhances this orientational deformation and also influence the particle distribution. This effect is illustrated by the curves in Fig.11 calculated with the aid of Eqs. (70)-(73). One sees that as $\tilde{V} = \mathrm{ED}$ raise, the particle concentration in the center of the cell begins to grow and reaches the maximum at V $\approx$ 4V. Further on, when the electric field causes substantial deformations of the orientational texture, the opposite tendency steps in–ferroparticles leave the central part of the cell and accumulate in those regions, where the conditions $\mathbf{m} \perp \mathrm{n}$ and $\mathrm{m} \perp \mathbf{H}_p$ of their minimum en-

ergy are favored. Due to that the concentration profile of FN changes. In the center of the cell the minimum of $f(z)$ occurs and instead of one maximum, two of them at equal distances from the middle turn up–see curves **3,** 4 in Fig.11. Apparently, the particle re-distribution affects the orientational profile $\vartheta(z)$ and, hence, the birefringence δ.

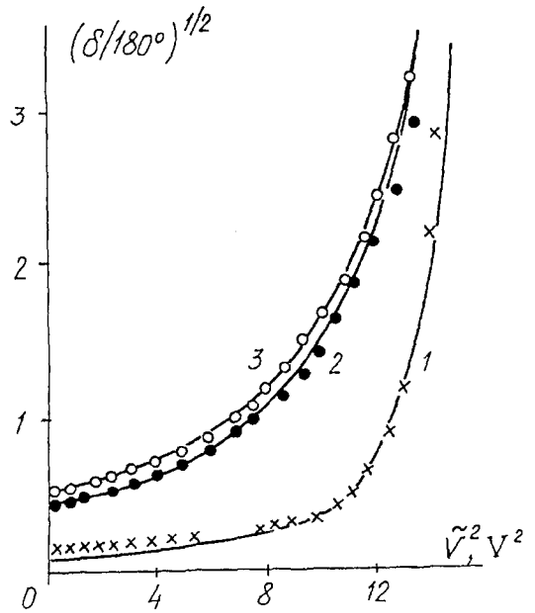

Figure 9: Initial parts of the voltage dependences of the electric-induced birefringence for given field-strength H and cell thickness D. Lines–calculations by Eqs. (70)- (74), dots–experimental data by Ref. [17]; H = 1.5 Oe and D = 222μm - (curve I and crosses), 4.0 Oe and 249 μm - (2 and black circles), 5.0 Oe and 234 μm - (3and empty circles).

It is important to emphasize that the correct interpretation of the experiment is impossible if the seggregation effect is ignored. Having not taken it into account, the authors of Refs. [17, 18] had been compelled to introduce (though lacking physical reasons) a strong dependence of the elastic modulus of the liquid-crystalline matrix upon the applied magnetic field strength. The direct attempt to fit the experimental points in the non-seggregation approximation has lead them to the following values (cf. the legend to Fig.9)

H, [Oe]	0	1.5	4.0	5.0
$K_3(H)$, $[\times 10^{-7} dyn]$	6.4	5.8	5.1	4.8

In fact, our consideration proves–see Figs.9,10–that the assurned function $\tilde{K}_3(H)$ is an artifact. The value of the elastic modulus K_3, once modified by the presence of the solid particle admixture, does not need to be changed in any field, providing the seggregation is taken into account.

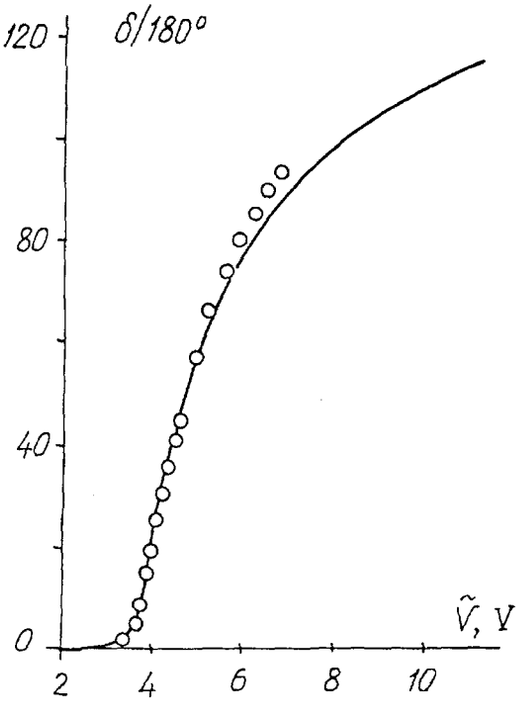

Figure 10: Voltage dependence of the electrically induced birefringence for the magnetic field strength H = 2.0 Oe and cell thickness D = 230μm. Line–calculation by Eqs. (70) - (74), dots–experiment by Ref. [18].

XII. Conclusions

We have discussed the principles of the continuum theory of ferronematics–the unusual anisotropic fluid media. Since FN is a heterogeneous substance consisting of at least two interacting phases, each of which is anisotropic, its correct model could be constructed only after thorough studies on the "microscopic", i.e., of the order of the particle size, spatial scale. The main subject of our interest are FN with soft anchoring of the nematic molecules on the particle surfaces. By now, this kind of FN is realized in thermotropic systems. The theoretical estimates and available experimental data shows that at present the notion of

thermotropic FN implies a siispension of prolate (rod-like) magnetically hard particles magrietized along their long axes. The mean particle dimensions are: length L $\sim 10^2$ nm and diameter $d \sim L/10$; their volume fraction range f $\leq 10^{-4}$. Such systems, once being rnagnetized, acquire and retain the spontaneous magnetization M $\approx I_s f \sim 10^{-1}$ G.

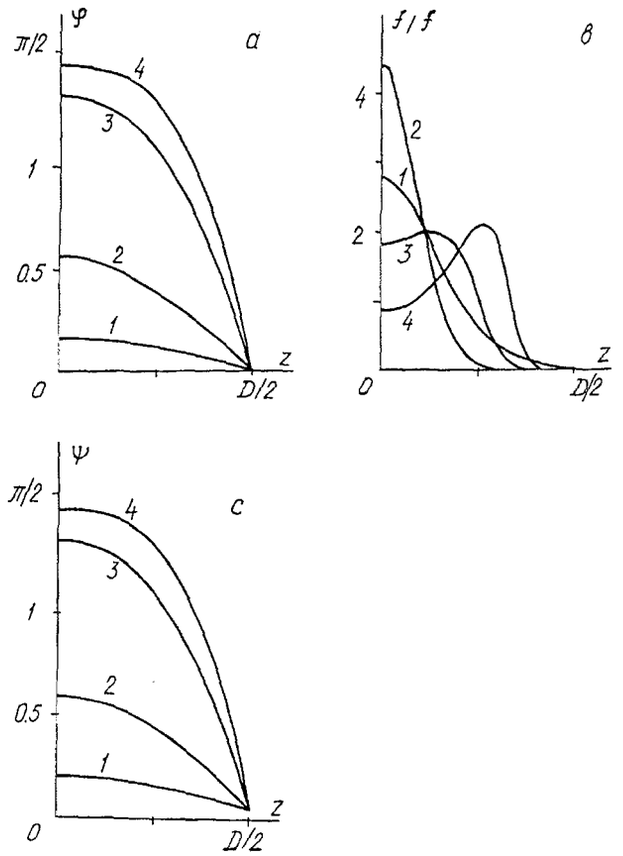

Figure 11: Orientation and concentration distributions in FN calculated by Eqs. (70)-(73) for H = 2.0 Oe and D = $230\mu m$. *The* electric voltage $\tilde{V}$ is 3.7V (curves **i),** 4.0V (*2*), 7.0V (*3*), 11.0V (*4*).

The equilibrium orientational state of FN depends upon the type and strength of the NLC molecules anchoring on the particle surfaces. For plain nematic carriers, like MBBA, providing the anchoring is homeotropic, it is inevitably soft. So, the basic internal structure of such a FN is the one, where director and magnetization vectors are perpendicular to each other. For the latter case we have developed a continuum description, v i ~ .derived the free-energy density function F–see Eq. (31). Description of stationary states is obtained by rninirnization of F or the functional $\tilde{\mathcal{F}}$ based on it. Two vector and one scalar equations following from relations $\delta\tilde{\mathcal{F}}/\delta\mathbf{n} = \delta\tilde{\mathcal{F}}/\delta\mathbf{m} = \delta\tilde{\mathcal{F}}/\delta f = 0$, together with the corresponding boundary conditions, form a closed set determining the equilibrium texture of FN, i.e., orientation $\mathbf{n}(r)$, magnetization direction $\mathbf{m}(r)$ and concentration $f(\mathbf{r})$ distributions for arbitrary values of the externa1 magnetic field.

By considering a number of particular cases encountered in experiinent, we have shown that the model developed herein, is capable to provide the non-contradictory interpretation, previously absent, of the existing experimental data. As to the latter, however, on close inspection one becomes aware that there is a great need in the properly defined methods to evaluate the material parameters of FN. The most essential ones of them are: the effective Frank moduli K_i, the amplitude of the anchoring energy W and the really acliieved concentration of single-clomain rnagnetic grains $\bar{f}$.

Acknowledgements

Tlie research work presented in this publication lias been made possible in part due to the Grant No. RMD 000 from tlie International Science Foundation which is thanlied by both autliors.

References

1. R. E. Rosensweig, Int. Sci. Tech., 48 (1966).
2. P. G. de Gennes, *The Physics* of *Liquid Crystals* (Clarendon Press, London, 1974).
3. J. Rault, P. E. Cladis and J. P. Burger, Phys. Lett. A, **32,** 199 (1970).
4. L. Liebert and A. Martinet, J. Phys. Lett. (France), 40, L363 1979; IEEE Trans. Magn., 16, 266 (1980).
5. L. Liebert and A. hl. Figueiredo Neto A. M., J. Phys. Lett. (France), 45, L173 (1984).
6. A. M. Figueiredo *Neto,* Y. Galerne, A. M. Levelut and L. Liebert, J. Phys. Lett. (France), 46, L499 (1985).
7. A. M. Figueiredo Neto and M. M. F. Saba, Phys. Rev. A, **34,** 3483 (1986).

8. T. Kroin and A. M. Figueiredo, Phys. Rev. A, ***36,*** 2987 (1987).
9. F. Brochard and P. G. de Gennes, J. Phys. (France), 31, 691 (1970).
10. Yu. L. Raikher, S. V. Burylov and A. N. Zakhlevnykh, Sov. Phys. JETP, 64, 319 (1986).
11. Yu. L. Raikher, S. V. Burylov and A. N. Zakhlevnykh, J. Magn. Magn. Mater., 65, 173 (1987).
12. S. V. Burylov, Yu. L. Raikher and A. N. Zakhlevnykh, in Static and Dynamic Properties of Magnetic Fluids, (Acad. Sci. USSR, Sverdlovsk, 1987) p. 12.
13. S. V. Burylov, A. N. Zakhlevnykh and Yu. L. Railther, in Magnetic Properties of Ferrocolloicls, (Acad. Sci. USSR, Sverdlovsk, 1988) p. 75.
14. S. V. Burylov and Yu. L. Raikher, Magnetohydrodynamics, 24, 25 (1988).
15. S. -H. Chen and N. M. Amer, Phys. Rev. Lett., 51, 2298 (1983).
16. S.-1-1. Chen and S. H. Chiang, Mol. Cryst. Liquid Cryst., 144, 359 (1987).
17. S.-H. Chen and B. J. Liang, Opt. Lett., 13, 716 (1988).
18. B. J. Liang and S.-H. Chen, Phys. Rev. A, 39, 1441 (1989).
19. S.-H. Chen and C. W. Yang, Opt. Lett., 15, 1049 (1990).
20. S. V. Burylov and Yu. L. Raikher, in: *Macromolecules, Colloids, Liquid Crystals and Biological Systems,* edited by H. Watanabe (Hirokawa Publ. Co., Tokyo, 1989) p. 29.
21. S. V. Burylov and Yu. L. Raikher, Phys. Lett. A, 149, 279 (1990).
22. S. V. Burylov and Yu. L. Railíher, J. Magn. Magn. Mater., 85, 74 (1990).
23. S. V. Burylov and Yu. L. Raikher, in *Proc. 2nd Internat. Conf. on Intelligent Materials,* edited by C. A. Rogers and G. G. Wallace. (Technomic Publ. Co., Lancaster, 1994) p. 247.
24. J. Cognard, *Alignment of Nematic Liquid Crystals and Their Mixtures* (Gordon & Breach, NY, 1982).
25. S. V. Burylov and Yu. L. Raikher, Phys. Rev. E, 49 (1994).
26. C. Y. Matuo, F. A. Tourinho and A. M. Figueiredo Neto, J. Magn. Magn. Mater., 122, 53 (1993).
27. L. D. Landau and E. M. Lifshitz, *Electrodynamics of Continuous Media* (Pergamon Press, New York, 1994) Chap. 5.
28. S. V. Burylov and Yu. L. Railther, J. Magn. Magn. Mater., 122, 62 (1993).
29. P. Pieranslti, F. Brochard and E. Guyon, J. Phys. (France), 34, 35 (1973).